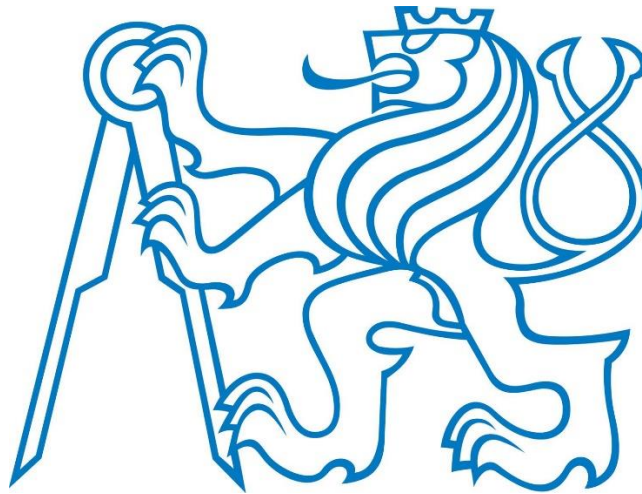


CZECH TECHNICAL UNIVERSITY IN PRAGUE

**Faculty of Electrical Engineering
Department of Microelectronics**



Master Thesis
The Structure of Quantum Dots
Struktura kvantových teček
Ruhani Dadashov

Study Program: Electronics and Communication

Supervisor: doc. RNDr. Jan Voves, CSc.

Prague 2021



MASTER'S THESIS ASSIGNMENT

I. Personal and study details

Student's name: **Dadashov Ruhani** Personal ID number: **490898**
Faculty / Institute: **Faculty of Electrical Engineering**

Department / Institute: **Department of Microelectronics**
Study program: **Electronics and Communications**
Specialisation: **Electronics**

II. Master's thesis details

Master's thesis title in English:

The Structure of Quantum Dots

Master's thesis title in Czech:

Struktura kvantových teček

Guidelines:

1. Study the quantum description of nanostructures, the applications of quantum dots and the software tool for quantum simulation of nanostructures.
2. Choose the suitable structure of the quantum dot and make the quantum simulation of its properties.
3. Discuss possible applications of the chosen structure and suggest its optimization.

Bibliography / sources:

- [1] E. L. Wolf: Nanophysics and Nanotechnology, Wiley, 2006
- [2] QuantumATK® and Sentaurus™ Materials Workbench Release Notes Version R-2020.09
- [3] A. Steane: Quantum Computing, Rep. Prog. Phys., vol. 61, pp. 117–173, 1998

Name and workplace of master's thesis supervisor:

doc. RNDr. Jan Voves, CSc., Department of Microelectronics, FEE

Name and workplace of second master's thesis supervisor or consultant:

Date of master's thesis assignment: **29.01.2021** Deadline for master's thesis submission: **21.05.2021**

Assignment valid until: **30.09.2022**

doc. RNDr. Jan Voves, CSc.

prof. Ing. Pavel Hazdra, CSc.

prof. Mgr. Petr Páta, Ph.D.

III. Assignment receipt

The student acknowledges that the master's thesis is an individual work. The student must produce his thesis without the assistance of others, with the exception of provided consultations. Within the master's thesis, the author must state the names of consultants and include a list of references.

Date of assignment receipt

Student's signature

Declaration

I hereby declare that this thesis is the result of my own work and all the sources I used are in the list of references.

In Prague, 20.05.2021

Signature.....

Acknowledgements

I am very thankful to doc. RNDr. Jan Voves, CSc., for his guidance, support, patience and always being with me in every step during writing this thesis. Without his help I would not have been able to find the right path and present any work. Besides, I would like to thank to my parents and my friends, Jamal Aslanov, Po-Wen Chen, Elmir Ismayilov and Ashish Garg, for their motivation and recommendations which was continuing during researching.

Abstract

This master thesis helps to get familiar with crystal defects and their electrical properties. In a theoretical part, there is a description of qubits and their working principle, the basics of quantum computers, the relationship between QPU and CPU, quantum dots, and their realization by different materials. The structure and energy levels of the nitrogen substitution atom in diamond and of the Nitrogen-Vacancy (NV) complex are analyzed. In the practical part, the base of software Synopsys QuantumATK that was used for this work is described. This program was used to create a pure diamond cluster with 250 C atoms, then to implement nitrogen, and, in the next step, to create NV defect in a diamond and in the last processed optimization of bond distances between atoms. The whole process was aimed to analyze quantum dots that could serve for qubits in quantum computers. DFT-PBE-SGGA method was chosen for this and tries were processed around this method. Obtained results from software QuantumATK were compared with other previous related works and the conclusion was mentioned at the end.

Keywords

NV defect in a diamond, carbon, quantum dot, quantum computing, QuantumATK.

Abstrakt

Tato diplomová práce seznamuje s defekty v krystalech a jejich vlastnostmi. V teoretické části jsou popsány qubity a princip jejich činnosti, základy kvantových počítačů, vztah mezi QPU a CPU, kvantové tečky a jejich realizace pomocí různých materiálů. Je analyzována struktura a energetické hladiny substitučního atomu dusíku v diamantu a komplexu dusík-vakance (NV). V praktické části je neprve popsán program Synopsys Quantum ATK, který byl nejprve použit pro vytvoření klusteru čistého diamantu tvořeného 250 atomy uhlíku, v dalších krocích pro implementaci atomu dusíku a NV defektu a nakonec k optimalizaci vazebných vzdáleností mezi atomy. Celý postup sloužil k analýze kvantových teček, které by mohly být použity jako qubity v kvantových počítačích. Získané výsledky byly porovnány s dříve publikovanými pracemi a v závěru kirátce zhrnuty.

Klíčová slova

NV defekt v diamantu, uhlík, kvantová tečka, kvantové výpočty, QuantumATK.

Acronym-list

QDs / QDots	Quantum Dots
NDD	Nanoparticle-based drug deliver
QPU	Quantum Processing Unit
QPC	Quantum Point Contact
CMOS	Complementary Metal–Oxide–Semiconductor
SQUID	Superconducting Quantum Interference Device.
SET	Single-Electron Transistor
ST	Singlet-Triplet
SEM	Scanning Electron Microscopy.
NV	Nitrogen-Vacancy
CNOT	Controlled NOT
GGA	Generalized Gradient Approximation.
LAPW	Linearized Augmented Plane Wave.
EHT	Extended Huckel Theory.
HF–LCAO–MO Orbital.	Hyperfine Field – Linear-Combination-of-Atomic-Orbitals – Molecular Orbital.
CNDO	Complete Neglect of Differential Overlap.
DFT	Density-functional theory.
LDA	Linear Discriminant Analysis.
UHF	Unrestricted Hartree–Fock.
SCF	Self-Consistent Field.
AM1	Austin Model 1.
MNDO	Modified Neglect of Diatomic Overlap.
FLAPW	Full-potential Linearized Augmented Plane Wave.
LSDA	Local Spin Density Approximation.
LCAO	Linear Combination of Atomic Orbital
MES	Molecular Energy Spectrum

DOS	Density of States.
PBE	Perdew-Burke-Erzerhof.
HOMO	Highest Occupied Molecular Orbital
LUMO	Lowest Unoccupied Molecular Orbital
SGGA	Spin-polarized Generalized Gradient Approximation

Table of Contents

1. Introduction	10
2. Quantum computing	12
2.1. Overview of the Quantum Computers.	12
2.1.1. Three Quantum power positions.	12
2.1.2. How do these machines work?	13
2.1.3. Quantum Processing Unit.	16
2.1.4. Qubits built on quantum dots.....	19
2.2. How do quantum dots work?	21
2.2.1. Theoretical model.....	23
3. Practical part.	27
3.1. Quantum Atomistic ToolKit.....	27
3.2. The structure of diamond.....	29
3.3. Diamond with nitrogen.	31
3.4. NV center in a diamond	33
3.5. Optimizing of NV center	35
Result and discussion	41
Conclusion	42
References	43
Appendix	47

1. Introduction

The whole world is trying to solve the most basic problems of Earth nowadays. The Covid-19 or other name Corona Virus might be the best example for now. The world is struggling with how to deactivate the functioning of the virus. The computation can help us. If we think of the inside of the virus, we can see the spiking proteins, and the proteins can be modeled and understood. Therefore, we could use them to explore different kinds of compounds that could deactivate how they function. Here supercomputers can come to help us. We can use these powerful computers to model this protein structure. Nowadays the foundation of computation consists of bits and qubits. Nanotechnology is one of the most popular fields of science in the last couple of decades. With the emergence of modern technologies and a better understanding of nano-science, this advancement has proved to be a boon, increasing its application in clinical, medical, biomedical, pharmaceutical science, and more specifically in the field of disease diagnosis, drug delivery, therapeutics, and imaging. Although nano-medicine has been extensively studied to overcome tumor-targeted delivery and treatment adaptive resistance, it is due to the advantages that nano-carriers provide similar multi-functionality enabling the deployment of drugs, affinity ligands, and the imaging parts are all within a single nanoparticle carrier, a targeted and traceable delivery system can be used. Among the nanoparticle systems, the most discussed are fullerenes, buckyballs, liposomes, carbon tubes, dendrimers, nanoshells, etc. And among them, Quantum dots (QDs) have gained popularity recently [1].

Quantum dots have a 1-10 nm nanoscale range and they are semiconductor crystals. Their energy levels can be controlled exactly since they have very small sizes as singular atoms. It can conduct or resist electricity depending on temperature and the purity of the semiconductor, due to they are made up of semiconductor crystals.

If thinking about colors that are made by QDs, the wavelength should be paid attention to. Most atoms have their own structure and therefore they can emit specific light, due to their structure. Quantum dots are not working with this rule. QDs can emit light but not depending on their elements or structure, depending on their sizes. The bigger QDs emit a bigger wavelength. The colors are depending on the wavelength, so this means that the largest crystal clusters will emit red light, and the shortest will emit blue, with all the other colors appearing in between. There are different bandgaps between different sizes of quantum dots [2].

The term quantum dot was discovered in 1986. They were first synthesized in a glass matrix by Alexey Ekimov in 1981 and in colloidal suspension by Louis Brus in 1983. They were first theorized by Alexander Efros in 1982 [3].

Quantum computers are believed to be able to solve certain computational problems, such as integer factorization (which underlies RSA encryption), significantly faster than classical computers. The study of quantum computing is a subfield of quantum information science. Paul Benioff describes the first quantum mechanical model of a computer. In this work, Benioff showed that a computer could operate under the laws of quantum mechanics by describing a Schrödinger equation description of Turing machines, laying a foundation for further work in quantum

computing. At the First Conference on the Physics of Computation, held at MIT in May, Paul Benioff and Richard Feynman give talks on quantum computing. Benioff's built on his earlier 1980 work showing that a computer can operate under the laws of quantum mechanics. The talk was titled "Quantum mechanical Hamiltonian models of discrete processes that erase their own histories: application to Turing machines" [4]

Complemented by the key advantages of optical imaging (high sensitivity, high resolution, multiplexing, and in particular low cost), QDots feature a combination of small size, versatile surface chemistry, and outstanding optical properties for real-time monitoring of otherwise "invisible" nano-carriers, while at the same time minimizing alterations in nano-carrier properties to authentically capture their behavior in biological systems. Quantum dots symbolize a versatile platform for the design and engineering of NDD vehicles [5].

In Fig.1.1, the top graphic shows the sizes of quantum dots under different methods. In middle graphics, some quantum applications are shown and they are categorized by quantum dots. Which sizes could be beneficial for some applications. There are 4 basic quantum dot methods: color center, shallow dopants, gate-patterned quantum dots based on silicon-on-insulator accumulation mode, and GaAs depletion mode, from left to right respectively [38].

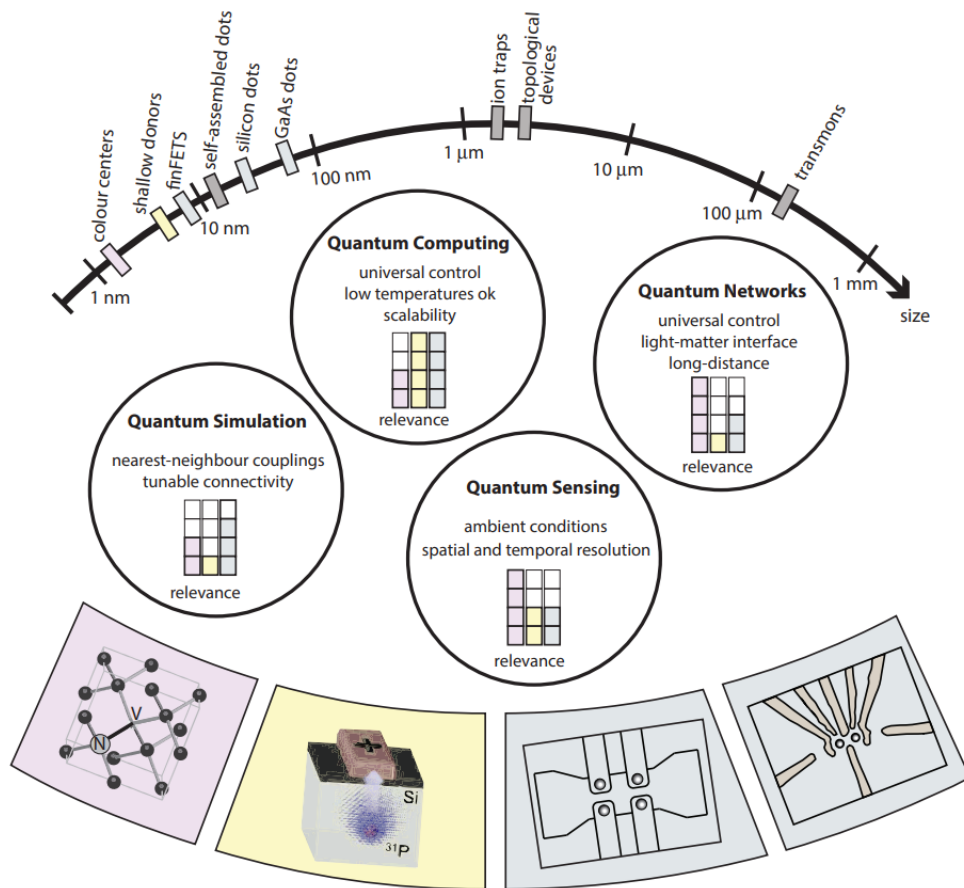


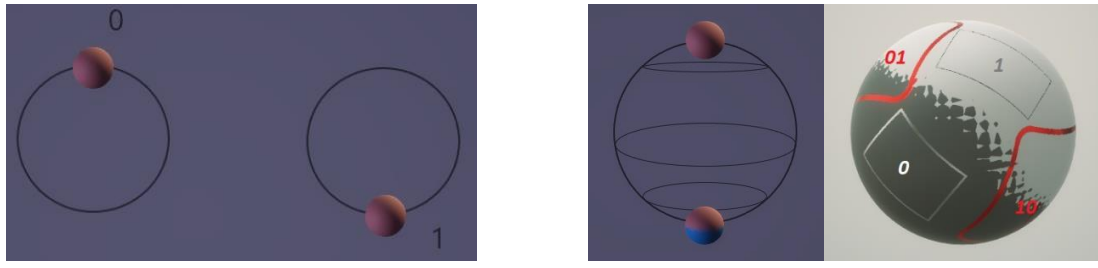
Fig. 1.1. Quantum dots size and their applications [38].

2. Quantum Computing

2.1. Overview of the Quantum Computers.

2.1.1. Three Quantum power positions.

There is a circle and two dots in Fig. 2.1.1 (a). When the dots are in the north pole that means it's a zero, when it is in otherwise it is one. That is a classical bit principle that is known by lots of people.



a)

b)

Fig. 2.1.1. (a) Classical bit definition and (b) Quantum Computer's bit definition [42].

The qubit is the unit of information in the quantum world. But in this sector, there are one and zero in one circle what this position is called superposition. And both the pole can be both of one and zero at the same time. Due to understand well the dots might be seeing like a Moon. The information can send by 0 or 1 or 01,10 at the same time Fig. 2.1.1. (b).

The Quantum can afford 3 super powers that are exhibited in the qubits:

The power of Superposition

The power of Interference

The power of Entanglement

In Fig. 2.1.2, on the left side, there is a superposition that consists of 0 and 1 on the poles. And the right side there is also a superposition that consists of the qubits what is called 'Moon' to understand. Due to interfered from the collection of both the one pole is got in a result. The states have interfered and that is called an Interference.

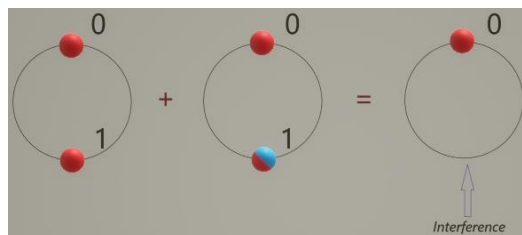


Fig. 2.1.2. Explanation picture of Interference of qubit [42].

How many states can be created? In a quantum create many numbers states can be created as is seen in Fig. 2.1.3. Red and blue dots where that end state cannot be described as the independent product of these five qubits in this case [6]. According to this principle, Table 1 is showing how many qubits equal to a classical bit.

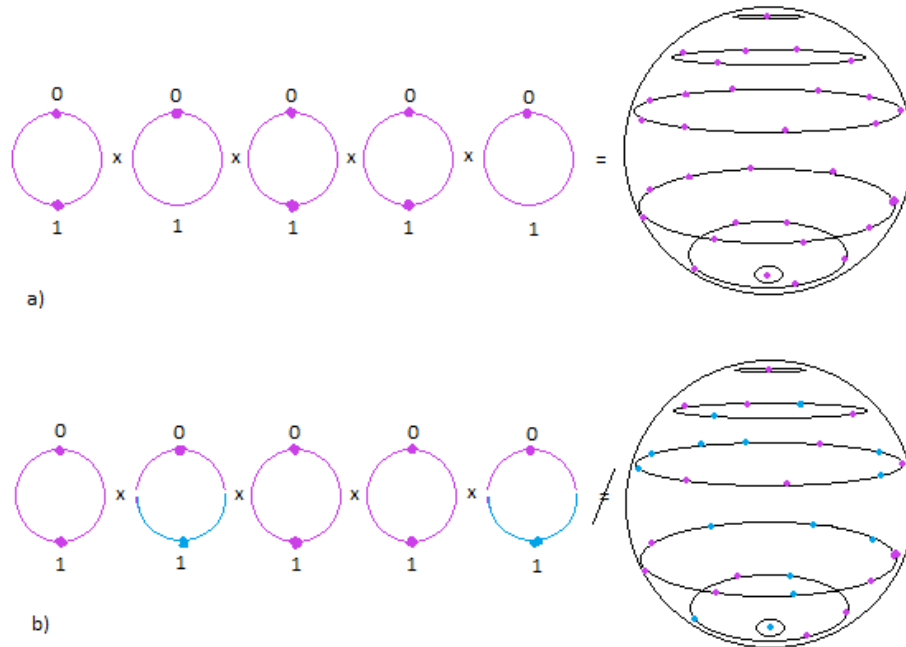


Fig. 2.1.3. (a) 5 independent qubits each with two states can create 32 states, $2^5=32$, (b) 5 entangled qubits combination do not give the same result [42].

2.1.2. How do these machines work?

Now quantum algorithms work principle is being focused on. Before, we imagine that we have 5 qubits with 2 states and after superposition rule 2 to the power of 5 is 32 states of dots. Then we have to encode the problem and inject data into the quantum machine. Encoding will happen via entanglement. It means some of the dots will change to other positions as seen in Fig. 2.1.4. The principle of interference comes from the fact that we can now take these states and combine them and interfere them with one another in such a way that we get to cancel things out and maximize the right answer. Many things fall away and the right answered gets maximized we perform a measurement and the result is gotten.

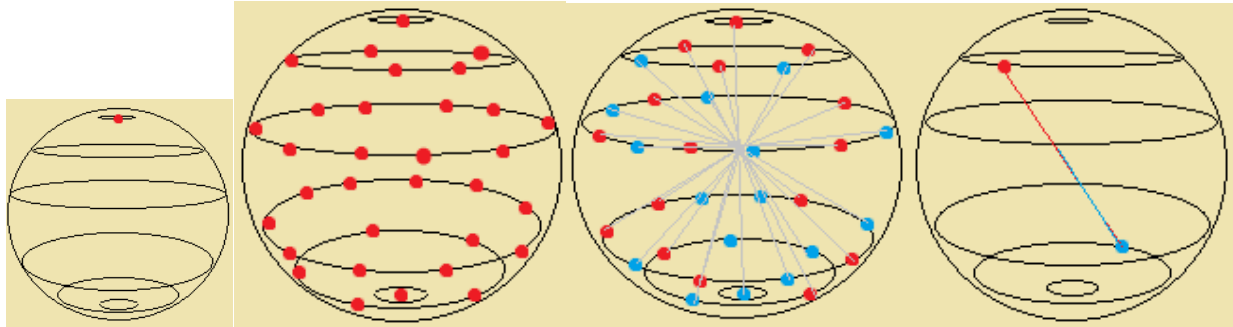


Fig. 2.1.4. Quantum algorithm work principle [42].

<i>Classical bits</i>	<i>Qubits</i>
512 bits	2
1024 bits	3
17 megabytes	20
17 gigabytes	30
More than all the atoms of planet earth	100
More than all the atoms in the universe	280

Table 1. How many classical bits are equal to quantum bit or qubit? [42].

As it's known, the classical computers are accessed we have to build and maintain it. But quantum computers are special machines that can be accessed by anyone in the world.

In the terminal classical zeros and ones are sending and they accept by laboratories of quantum computers. These zeros and ones are converted to microwave pulses they operate about five gigahertz. After that, these pulses are being sent to a dino cryostat that operates at about -273 Celsius temperature and they get to use those microwave pulses to manipulate these qubits to perform those superposition, entanglement, and interference operations and then return the result to the user Fig.2.1.5. Surprising is that all of the procedure could be done by our classical computers [42].

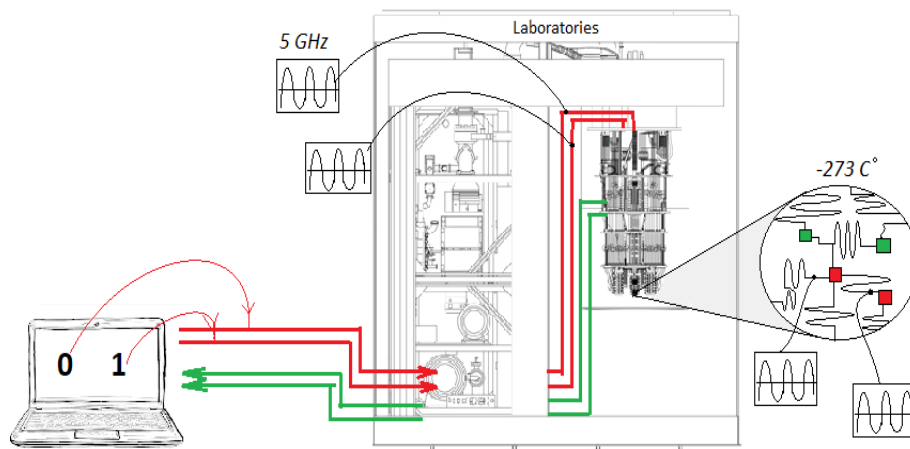


Fig. 2.1.5. The principle of converting of classical bit to qubit [42].

The Quantum circuit is the unit of value for the quantum business. A qubit is a unit of information but a circuit is the unit of computation. The instruction of the circuit is consisting of qubits and gates that are special for quantum computers and we can make our own codes to create some businesses with them. These gates can be understood like ‘and or nor...’ in a classical computer Fig.2.1.6.

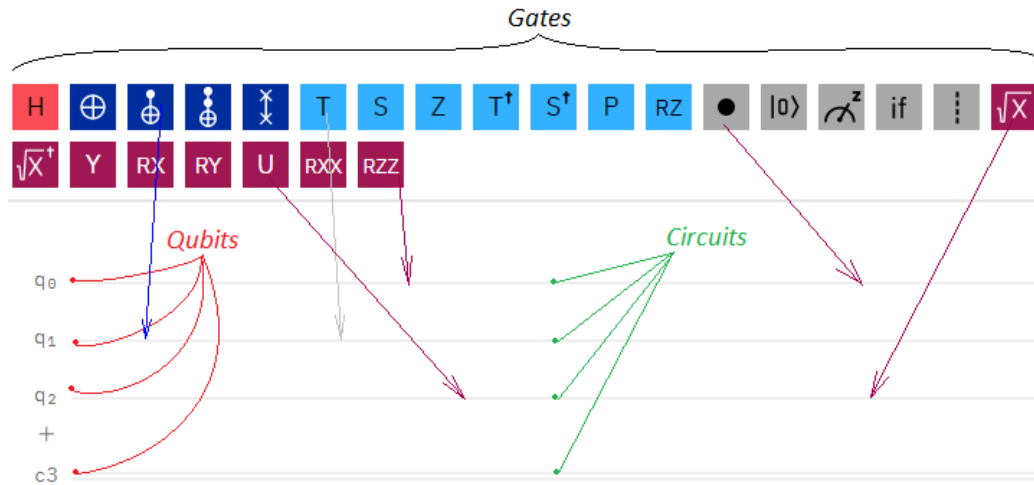


Fig. 2.1.6. Modern code writing way for quantum computers [42].

These gates or operations are very ideal for doing the rotation of the “moon” between one and zero. Paying attention to the comparison between a classical circuit and a quantum circuit.

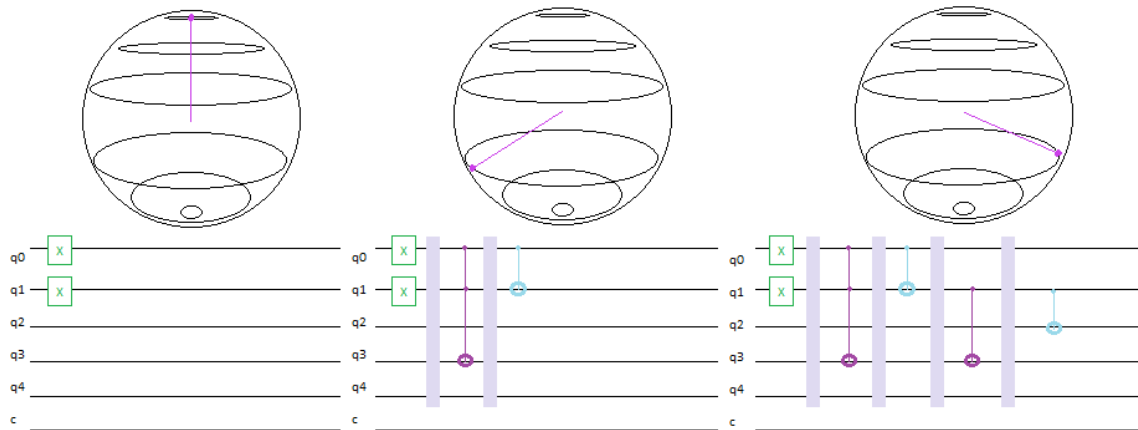


Fig.2.1.7. The working principle of coding according to situation of qubits [42].

In the classical circuit, a blue face that can be zero or one at the same time with pink cannot be seen. But in quantum circuits, the gates can operate orders at one time and using all of the circuits. In the first step, the complex superposition principle is working, when the orders are going to up, the interference and entanglement principle is working for every “dot” that comes from superposition and occupies every circuit. And this allows us in one order we can use all circuits, get result super-fast Fig.2.1.7.

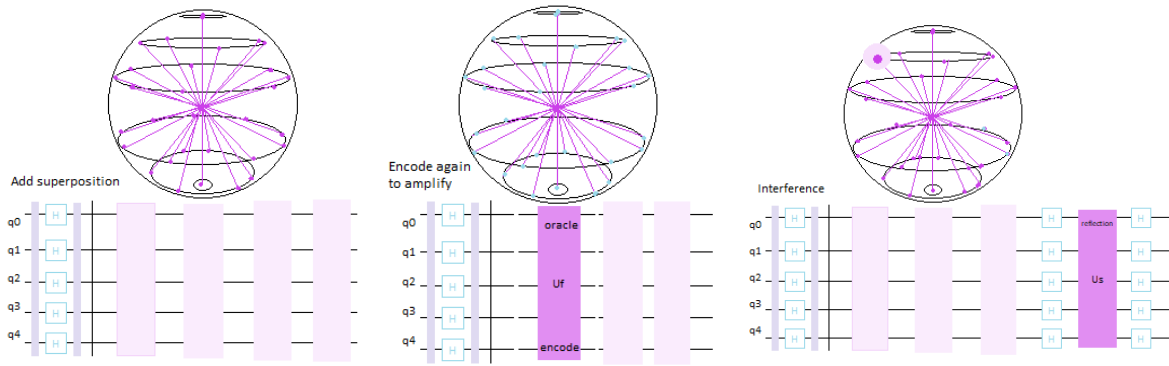


Fig.2.1.8. Informing of crucial information in interference step [42].

In this interference process, the “moon” is bigger and it is telling that some important answer is converted Fig.2.1.8. These circuits allow us to make fix codes for and operations for different applications. There are some applications in the below with fix operations Fig.2.1.9.

1. Inverse Quantum Fourier Transform
2. Chemistry Circuits
3. Quantum Fourier Transform
4. Multi-controlled NOT-gate
5. Weighted Adder
6. Logical OR [7].

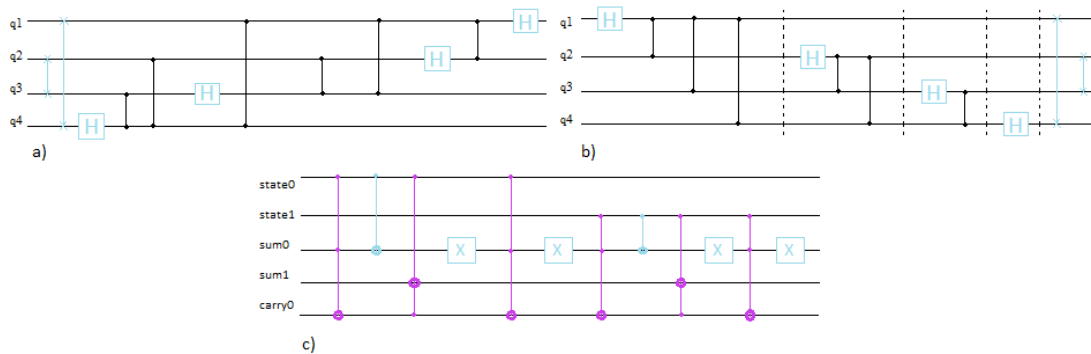


Fig. 2.1.9. Applications with fix operations. (a) Inverse Quantum Fourier Transform, (b) Quantum Fourier Transform, (c) Weighted Adder [42].

2.1.3. Quantum Processing Unit.

QPU is ordered to be a calculational principle that is using for quantum computing to make the performance of a task. This processing unit is a very important part of quantum mechanics which has several unmatched skills that other parallel computer platforms do not have. In firstly, a QPU collects computational parts in the format of a quantum mechanical state. Quantum states must be calculated as the data processed by the QPU and at the same time, it is defined as a unit vector in a finite-dimensional Hilbert space. Qubit is most periodically used in the example which has a

state on a two-dimensional Hilbert space. In quantum physical systems, these states are stored. Due to understand well, a quantum register is defined as a place which has the exact address of two-level quantum physical systems. The individual regime of the register is imagined as a quantum register element and each register element that can hold qubit information is accepted. The size of the register might be accepted by the number of qubits which it could hold, n-qubit register, for example. The computational space depends on a quantum register that scales exponentially with its size. For example, the n-qubit register could be the face of all 2^n computational states like the n-bit register. However, due to the use of a phenomenon is known as entanglement, the quantum register is also capable of representing these states' superpositions at the same time, and this is not formal to the classical computer system. Substantially, entanglement specifies the value of each register element and with this ability, it could describe states of register simply. This is too opposite to classical computers of computation and this could be given a description of specialization which is named the "inherent parallelism" of quantum computing. Most quantum algorithms use this super correlation during calculation, and the advantage of entanglement is used to get a time advantage with its speedups. The gates are used for operations on the quantum registers. Quantum gates make communication with well-defined transformations of the computational states like traditional computing. The operations move to multiply for calculation effectively when the register starts to be prepared in a superposition state. It could be accepted SIMD processing like a quantum variant.

SIMD processing: Single instruction, multiple data. In this processing, there is more than one element in a computer that they might compute multiply. The results could be gotten at different times, but calculations are processed at the same time.

But quantum computing uses the gates on two sides: either projective measurements or unitary transforms of the register elements. Only the last gates can prepare the value of the result like a classical value, for example, 0 and 1 for each register element. The unitary gate of the value of the register remains in a computational states' superposition and it serves as an intermediate computation. In a conclusion, when a projective computation gate is applied to the register, at that time, the solution to computation is recovered. The bit series of results should be stocked in a classical register in the QPU Fig.2.1.10.

The registers and gates are defined by quantum computational models within a QPU that how they realize quantum computation. All models show differential with the hardware implementations and principles of operations when these models offer the same computational power from a complexity perspective. The quantum circuit models' work principle is related to the classical circuits, for example, due to want to make series computational states, the models apply different gates. The adiabatic quantum computing models have the aim to improve computational state while using time-dependent and continuous transformation of interactions between register elements. For example, modern special-purpose processors in the adiabatic quantum computing model use a single offer about the duration to perform quantum optimization. The quantum physical degrees of freedom defining register elements are required by QPUs in all computational models [43].

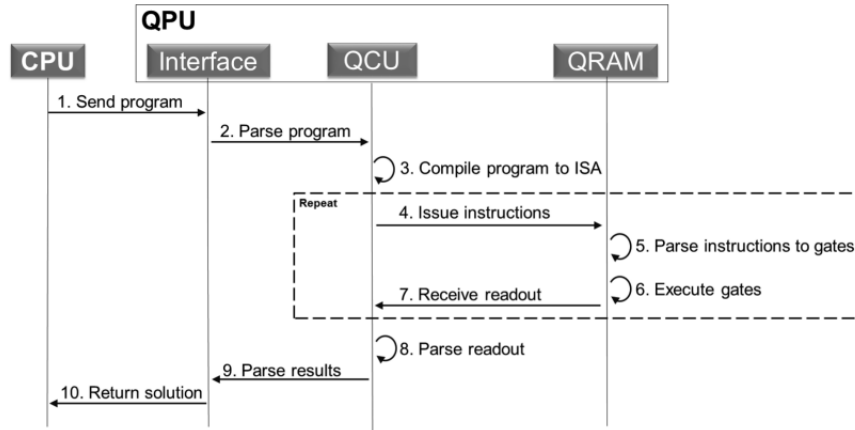


Fig. 2.1.10. The diagram shows relationship between CPU and QPU [43].

We are using CMOS transistors on a classical computer by coding 0 and 1. But in Quantum Computers we are not able to make codes with normal transistors, Superconducting Quantum Interference Device (SQUID) is used for QC. Coding is proceeding by “+1” and “-1”. The structure of superconducting qubit encodes 2 states as tiny magnetic fields, which either up or down. They are corresponding by this method and qubit can choose one side between them. That is letting us put qubit into superposition Fig.2.1.11. (a, b). The material of SQUID is niobium which the metal is cooled down, it becomes what is known as a superconductor and it starts to exhibit quantum mechanical effects.

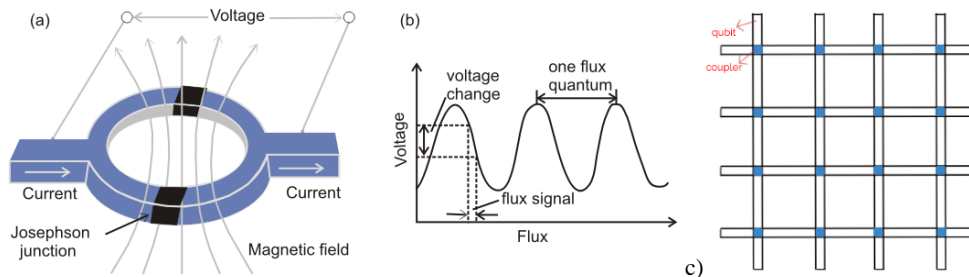


Fig.2.1.11. (a) Superconducting Quantum Interference Device, (b) graph of Voltage-Current [44], (c) relationship between qubits and couplers [45].

The qubits then must make a connection between them to forward information. This connection is made by couplers. The couplers are also made from superconducting loops. By putting many such elements (qubits and couplers) together, we can start to build up a fabric of quantum devices that are programmable Fig.2.1.11(c).

There is circuitry that surrounds the coupler and qubits. This circuitry is formed from the Josephson junction which is the main part of making the direction of information through qubits. This circuitry is forming addresses on both sides of qubits. And the information is shared by magnetic fields to these addresses and stores that information in the magnetic memory local to each device.

Additionally, there are readout devices attached to each qubit. During the computation, these devices are inactive and do not affect the behavior of qubits. After the computation has finished, and the qubits have settled into their final (classical) 0 or 1 states, the readouts are used to query the value held by each qubit and return the answer as a bit string of 0's and 1's to the end-user.

In Fig.2.1.12., there is a layout of the actual circuit drawn by the CAD program. We can see the pink lines what are the qubits. Yellow dots are the Josephson junctions and the control circuitry lines which carry currents to the programmable are indicated by the green features. It is not definitely different than classical processing units, QPU has no large area of memory [8][45].

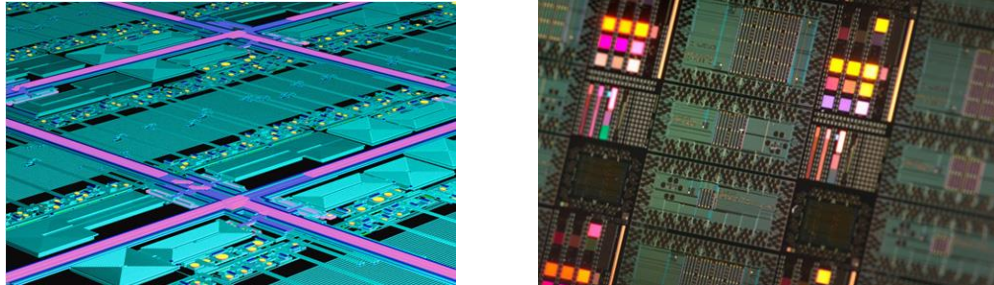


Fig. 2.1.12. The views of inside design of QPU [45].

2.1.4. Qubits built on quantum dots.

The semiconductor quantum dot is also called an ‘artificial atom’, which is made inside a semiconductor that can catch a few or even a single electron and these dots are three-dimensional potentials. GaAs and Si are used for QDs mostly. I(dot) or I(QPC) can be used for the readout of charge states. If an electron makes tunnels the inside or out of QDs, this happen can change the conductivity of quantum dots. After this process, we might see the single-electron regime in a quantum dot.

Si is more useful than GaAs for the spin qubits. Since it can reduce the magnetic noise and it is weak hyperfine interaction. Si/SiGe heterostructure or CMOS channel is a good opportunity for silicon quantum dot. There are 2 categories in Si/SiGe: undoped and doped (which is similar to GaAs) quantum dots. It is shown in Fig.2.1.13. (a).

According to the scanning electron microscope (SEM), an overlapping-gate device is shown in Fig.2.1.13. (b). The lower half of the device is a single quantum dot. The upper half of the picture shows us a single-electron transistor that serves as a charge sensor that can be related to the QPC channel. Electrons could come to the source and drain by lead gates (green). The lead gates (green) introduce electrons from source and drain, and the SET is formed via two barrier gates (orange) and the quantum dot is formed by restriction gates (blue), plunger gates (red), and barrier gates (orange) [10].

In Fig.2.1.13. (c), it is seeming the barrier gates are surrounded by very thin insulating oxide (silver gray). In the last times, such types of gates are used in Si/SiGe quantum dots, and it shows potential elastic control [9][10].

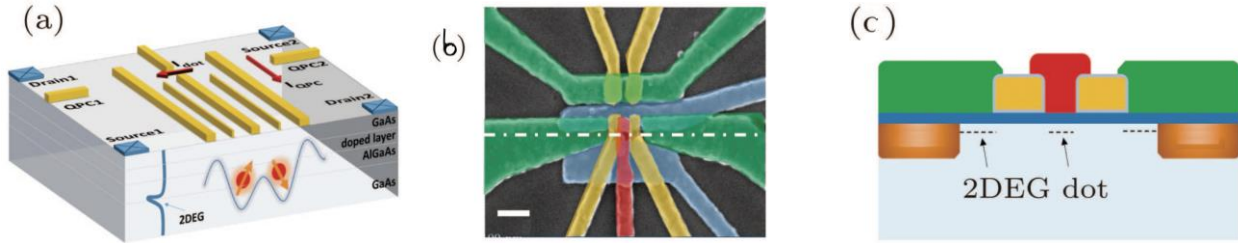


Fig.2.1.13. Device structure of the semiconductor quantum dot [10].

We can see some methods to form a qubit: Spin qubit, Singlet-triplet qubit, Exchange qubit, Exchange-only qubit, Charge qubit, Resonant exchange qubit, Hybrid qubit, Long-range coupling of qubits [10].

Charge qubit. If we want to directly form a qubit, we will use the charge state of a double quantum dot. Charge qubit can be described by the occupation of surplus electron on the left or right dot with electrochemical of E_L and E_R . In 2013, Guo's group actualized the GaAs quantum dot for universal control of charge qubit. In 2015, this group showed GaAs quantum dots with a clock speed which was up to 6 GHz. We can see Controlled-NOT ideal gate result in Fig.2.1.14. [11].

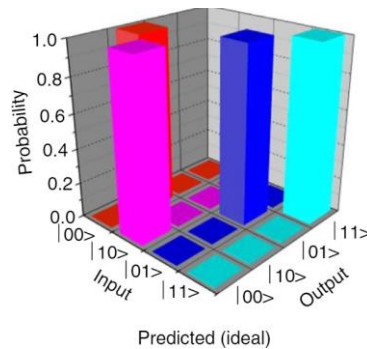


Fig.2.1.14. The truth table of Controlled-NOT operation [11].

Spin qubit. In 1998, Loss and DiVincenzo realized qubit by single electron spin first time. We can explain spin is showing us the magnetic influence on a particle. Therefore, if we compare it with charge qubit, we can agree spin qubit is less impressed magnetic, charge noises than charge qubit. And it makes more decoherence time on spin qubits [12].

Singlet-triplet qubit. Petta used two spins that have exchange interaction between and called it singlet-triplet qubit (ST). Due to making two-qubit gates on ST qubits, it should be used adjacent ST qubits that are coupled capacitively. Due to the Pauli exclusion principle, different states charge different electric fields on the other in the first qubit. And it can help to shift in the motion frequency of the second qubit, therefore there is the rotation of the mechanism conditionally. This way was improved by Yacoby's group that was an entanglement of ST qubits on their devices, in 2012 [12][13].

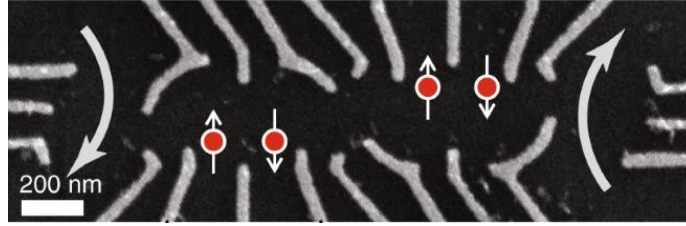


Fig.2.1.15. SEM image of a device for two ST qubit gate. The axes are current path for charge sensing [13].

2.2. How do quantum dots work?

We cannot think of Quantum Computers without qubits that have to be controlled in such ways. One of the ways is controlling qubit by electromagnetic waves. In this variant, disturbance can be defended, but the disadvantages of this method are qubits have to be moved in spatial coordinates to manage their position. This method can be realized by ion traps with high effort [14][15].

A more appropriate variant is a solid-state solution that can be connected more easily with CMOS technology. In the solid, quantum objects are restored automatically and even in a bad situation, the position of objects can be maintained by qubits. ^{12}C diamond crystal can be used in this method and defect of the inside may be appropriate for a realizing of qubit [15][16][17].

At room temperature, the defect center can manage their spin states. Nitrogen-Vacancy or NV center might be a good example for the defect center. The creation of defect consists of the neighbor vacancy with nitrogen atom and a nitrogen atom which can be one ^{14}N or half of ^{15}N [15][18].

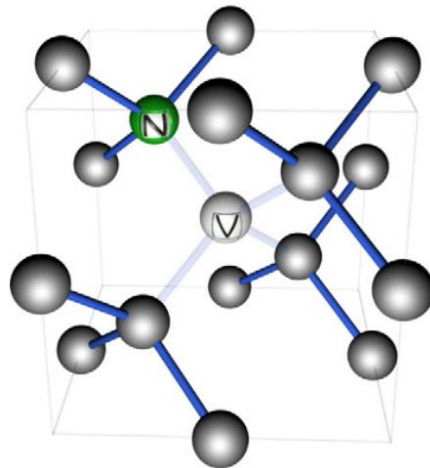


Fig. 2.2.1. Structure of the nitrogen–vacancy (NV) center [19].

At this point, we can ask why we are using NV centers for qubits to realize spin state. Since we have other centers such as SiV, ST1, or L2 centers. But long coherence time is seen in NV centers [20]. Triplet state can be realized by negatively charged defect and we can see this state in both excited and ground state. Three situations are seen for quantum number, “m”: $m = 0, -1, +1$. Transition rates are stronger for $m = 1$ and $m = -1$ than for $m = 0$. With 98% probability, the spin polarization is achieved after some small excitation cycles. Conversion of $m = 0$ (qubit $|0\rangle$) to $m = -1$ (qubit $|1\rangle$) is realized by π -pulse [15][21].

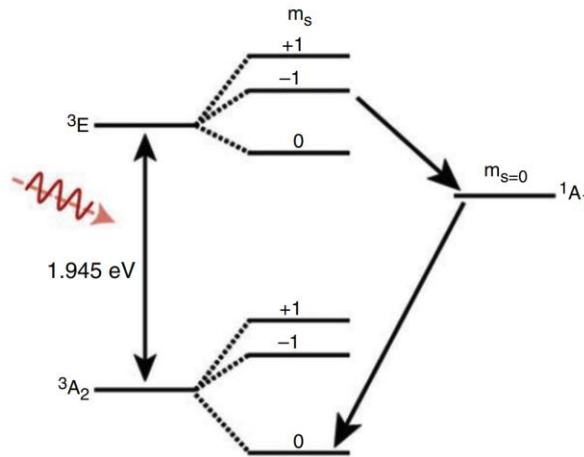


Fig.2.2.2. Energy level scheme of the NV centers [22].

The local shift of the Fermi level, unwanted electrical properties such as unsaturated electrons and nuclear spins could be seen due to defects. The electron spins are important for the color centers since the sequence of relationships is a couple of nanometers and it strongly affects coherence times [15]. The defects cannot be destroyed, if these defects extended by free electrons which are realized via laser pulse in the conduction band. Removing of vacancies that are electron traps, for example, can be realized via implanted NV center [23].

Under the high resolution, ion implantation and nitrogen implantation inside of NV centers gave us good results for the properties of spin. The switching of the spin state of the NV center can be controlled by microwave pulse which is called π -pulse. The CNOT gate is represented by π -pulse [15][24].

Up to 30 spins can control high-quality and entanglement quantum algorithms in chips up to 10 qubits. The qubits with diamond have 99.995 % performance for single-qubit gate and 99.2 % performance has for double qubit gates [25].

2.2.1. Theoretical model?

Due to make a quantum dot, the one-carbon (C) atom is changed by one nitrogen (N) and realized vacancy (V) for one carbon atom more. This process is realizing inside of diamond molecule which consists of 64 C atoms in Fig.2.2.3.

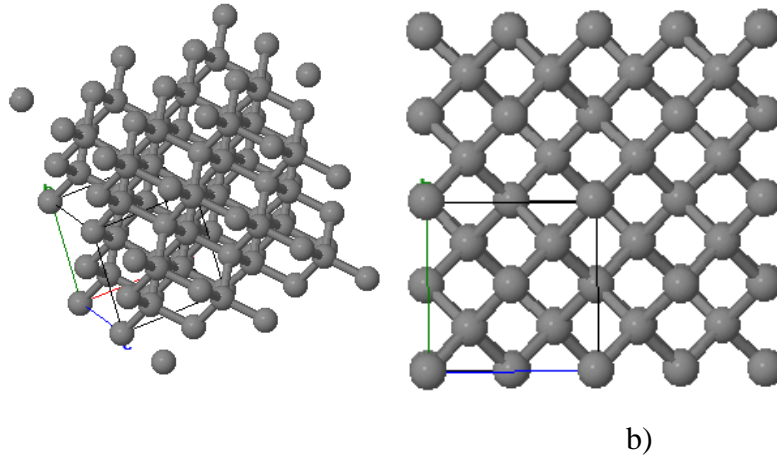


Fig. 2.2.3. The structure of diamond models with 64 C atoms. (a) 3D model of structure. (b) The view in [001] direction of structure [26].

Due to getting vacancy, it is enough to remove one C atom from the cluster. This vacancy should be a neighbor of the N atom. Nitrogen - vacancy is chosen in the center of the diamond cluster. This means this method will be made on 63 C atoms as is shown in Fig.2.2.4.

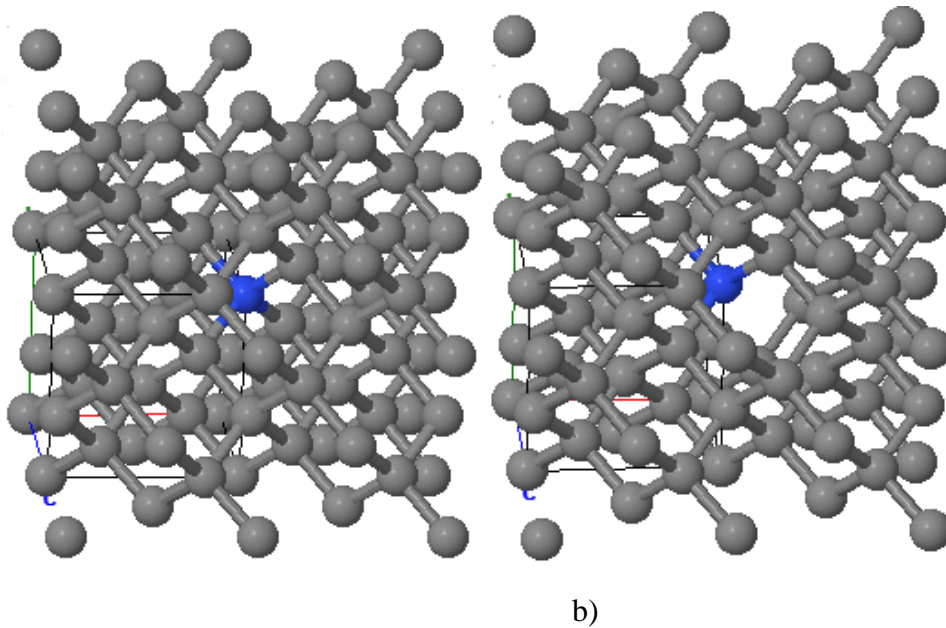


Fig. 2.2.4. (a) The diamond structure which one C changed by N. (b) The diamond structure with NV center [26].

Due to getting minimum energy for the system, the lattice relaxation is paid attention to with the use of the pseudopotential method. The atoms can be moved which are located in the very near of vacancy. The result of the optimization is used for electronic structure calculations [27].

Generalized gradient approximation is used for the calculation of self-consistent spin-polarized to check the effect of a single N-V defect on the electronics diamond structure under the full-potential linearized by the augmented plane wave method. In a small region around the atom, the relativistic contact contribution is determined by averaging electron spin under the LAPW method [28].

According to the change of atom, the lattice gives deformation. A small piece of center keeps its axial symmetry. The distance between atoms is shown before and after optimization in Table 2 and Fig.2.2.5 (a). After optimization, the average of increasing distance between N-C (1,2,3) is 8% approximately. The density of States for NV center for spin-up and spin-down is shown in Fig. 2.2.5 (b) [27].

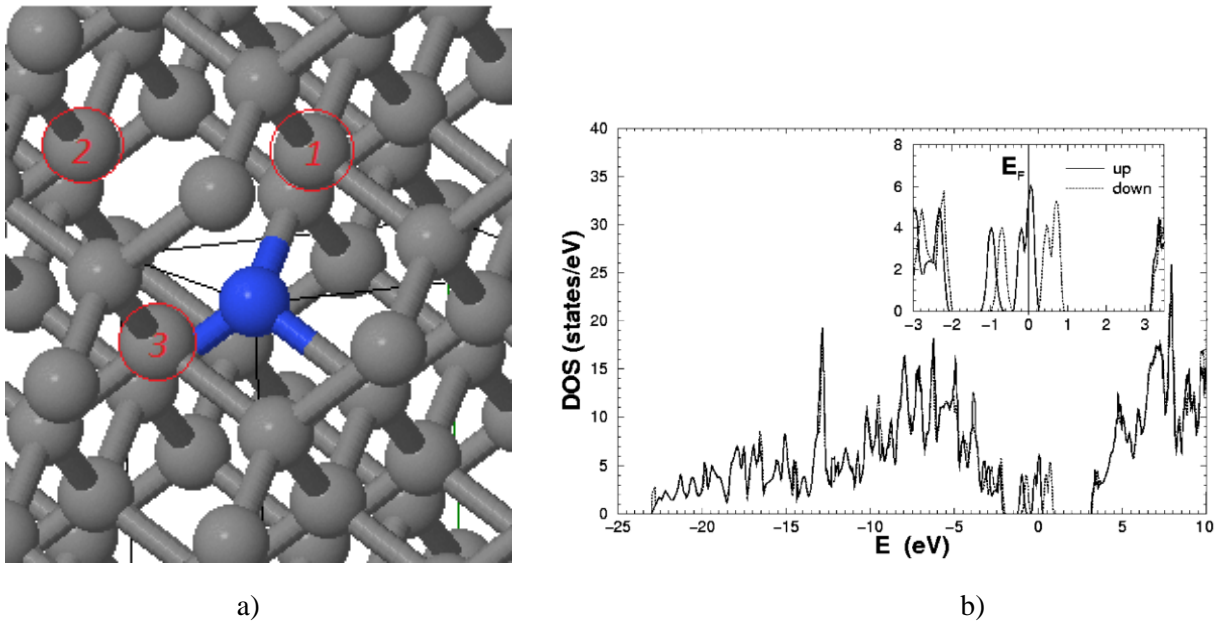


Fig. 2.2.5. (a) The blue atom is N and C atoms which is numbered are nearest neighbor atom with vacancy, (b) DOS for NV center of Diamond [26].

Atomic pair	Distance (Å)	
	Before optimization	After optimization
N—C(1)	2.5228	2.7230
N—C(2)	2.5228	2.7227
N—C(3)	2.5228	2.7223
N—C(13)	1.5372	1.5010
N—C(14)	1.5372	1.5016
N—C(15)	1.5372	1.5013
C(1)—C(4)	1.5372	1.5081
C(1)—C(5)	1.5372	1.5073
C(1)—C(6)	1.5372	1.4832
C(2)—C(7)	1.5372	1.5053
C(2)—C(8)	1.5372	1.4840
C(2)—C(9)	1.5372	1.5086
C(3)—C(10)	1.5372	1.4841
C(3)—C(11)	1.5372	1.5085
C(3)—C(12)	1.5372	1.5057

Table 2. Distances between atoms before and after the optimization. C (4,5,6,7,8,9,10,11,12,13,14) are other neighbor atoms around the N-V center [27].

In some other method, the GGA-DFT-FLAPW method used for only implementing N in a pure diamond. This method shows 28% enlargement in bond distances between C-C. If paid attention to energy levels of nitrogen impurity in diamond for 64 atoms, there is an impurity state of 1.89 eV below the conduction band for spin-up, 1.07 eV below the conduction band for spin-down in Fig.2.2.6 (a). There are also DOSs for pure diamond and diamond with nitrogen in Fig.2.2.6 (b, c respectively) [34]. And other calculation methods for the average result of the distance between atoms are shown in Table 3.

In different research, GGA of Perdew-Burke-Erzerhof and non-relativistic Trouiller Martins pseudopotentials method is used for NV center in diamond bulk. After computation, the HOMO-LUMO energy level index result for spin-up and spin-down is shown in Fig. 2.2.7. There are a couple of bulk diameters and their different results are shown. HOMO-LUMO energy gap could be different for distinct defects. Therefore in Fig. 2.2.8., the bars show the different values of the HOMO-LUMO gap for spin-up and spin-down. After computation, the average bond size in a center is 1.4651 Å and in a surface, it is 1.4656 Å [39].

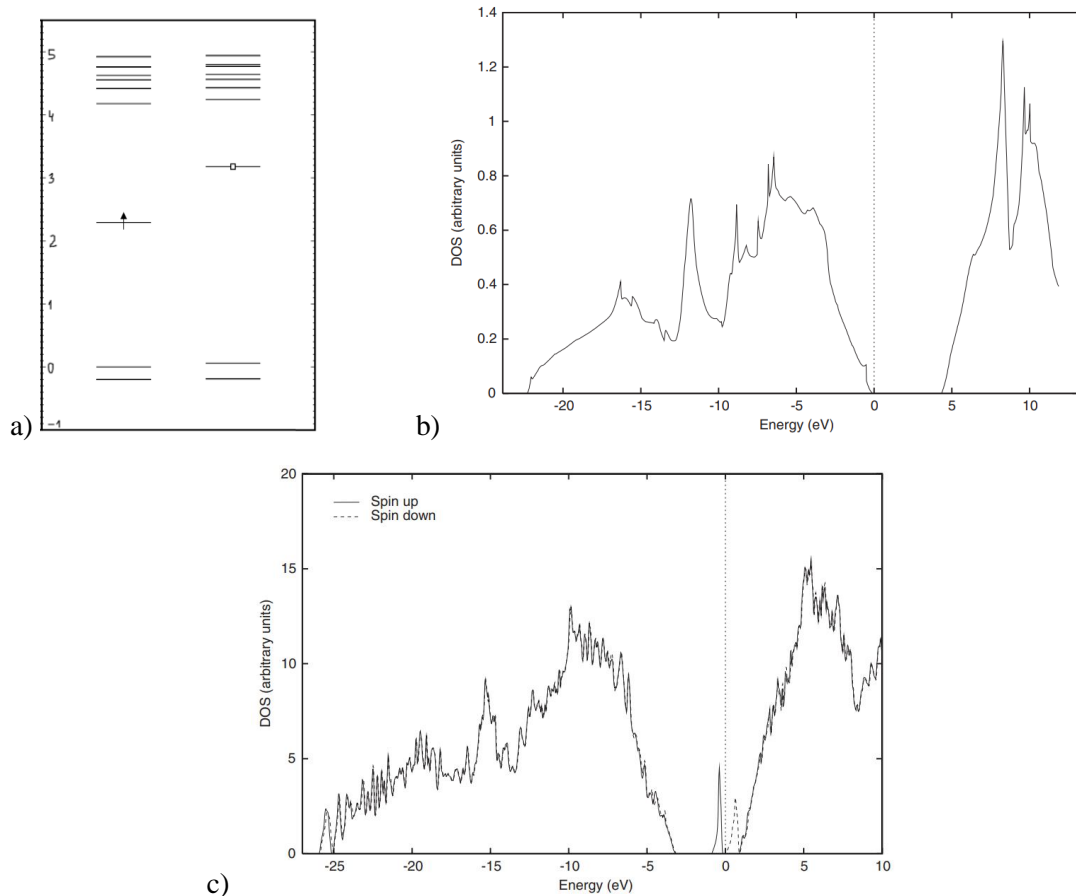


Fig. 2.2.6. (a) Molecular energy levels for N in diamond, (b) DOS for pure diamond and (c) DOS for Nitrogen impurity in Diamond [34].

References	Method	Elongation of N-C bond	References	Method	Elongation of N-C bond
1.	EHT	26%	7.	DFT, plane waves (periodic)	25%
2.	HF-LCAO-MO (finite cluster)	~5%	8.	DFT, LDA (finite cluster)	28%
3.	CNDO (finite cluster)	5-10%	9.	MNDO	0%
4.	CNDO (finite cluster)	24-25%	10.	UHF AM1 (96-atom supercell), spin polarized	0%
5.	UHF-SCF (finite cluster) spin-polarized	19%	11.	DFT-LSDA (finite, 165 atoms), spin polarized	32.9%
6.	DFT, LDA (finite cluster)	0%	12.	FLAPW GGA (8-atom supercell), spin polarized	21.2%
			13.	APW + lo GGA (64-atom supercell),	28.1%

Table 3 [34]. The results of different method for optimization of distance between atoms. 1 – [29], 2 – [30], 3 – [31], 4 – [32], 5 – [33], 6 – [34], 7 – [35], 8 – [36], 9 – [37], 10,11,12,13 – [34]. (3) This method is calculated for Vacancy in diamond, (4) this one is calculated nitrogen and N-V complexes in diamond.

3. Practical part.

3.1. Quantum Atomistic ToolKit

In the practical part, the calculation is processed by QuantumATK software through Synopsys. QuantumATK gives the chance to simulate the atomistic nanostructures different quantum approaches:

- Semi-Empirical Tight Binding
- Classical Potentials
- Density Functional Theory
- Non-Equilibrium Green's Functions

Electronics, mechanical, optical, and other properties of materials and nanostructures can be calculated by QuantumATK. In advanced data analysis, Python programming is used to make easy complex workflows efficiently. And also VASP, LAMMPS, ABINIT, QuantumEspresso could be producing the output results for calculations, structures, geometries that are built by QuantumATK Virtual NanoLab. The results, input files might be in a Python file, JPEG, or PNG, Notepad formats.

The general process could be divided into 3 main sections:

- Builder
- Script Generator
- Job Manager

Atoms, bonds, molecule, bulk, the lattice is building in the first step, in the builder (Fig.3.1.1). Appropriate atoms are chosen from an included database, then the number of atoms is figured out by "Bulk Tools". After that, the configuration could be kept like bulk or could be changed to the molecule. The last step is passing to the second main step by choosing Script Generator.

The very important part is Script Generator for the computation (Fig. 3.1.2). Firstly, the structure needs to be chosen by the right Calculator. Then the right sections are choosing from the Analyzing for the right aim. If the structure needs optimization after changing some atoms for example and due to comparing the before and after optimization, the right section should be chosen from Optimization as well. After whole these processes, the Job Manager section could be chosen for the next key step.

In the last step (Fig.3.1.3), the file location is chosen, and the run is started. After some hours, the result would be able to get if the mistake is not made [37].

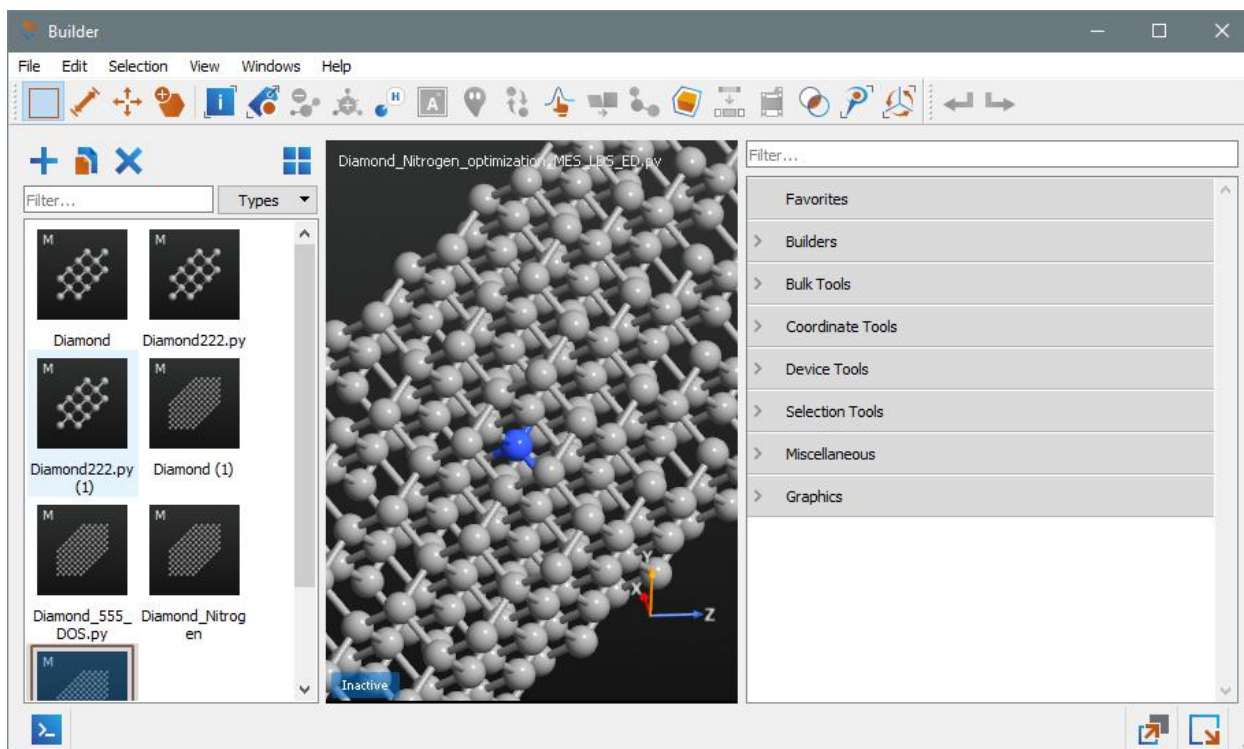


Fig. 3.1.1. Builder, QuantumATK.

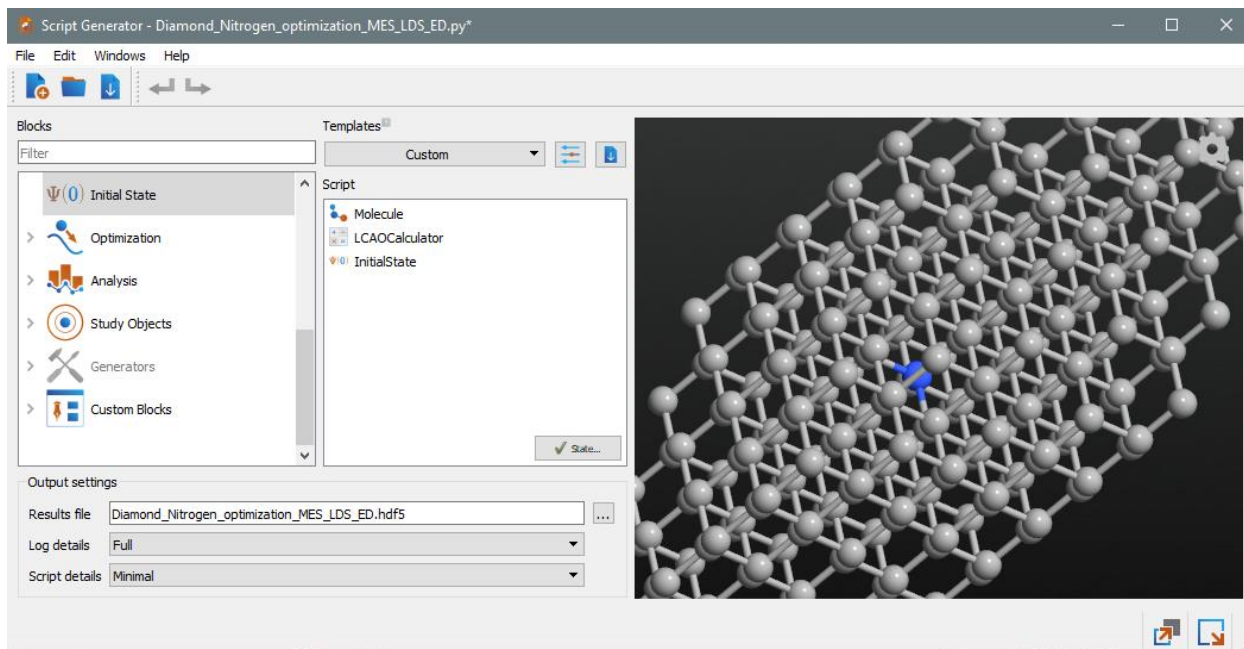


Fig. 3.1.2. Script Generator, QuantumATK.

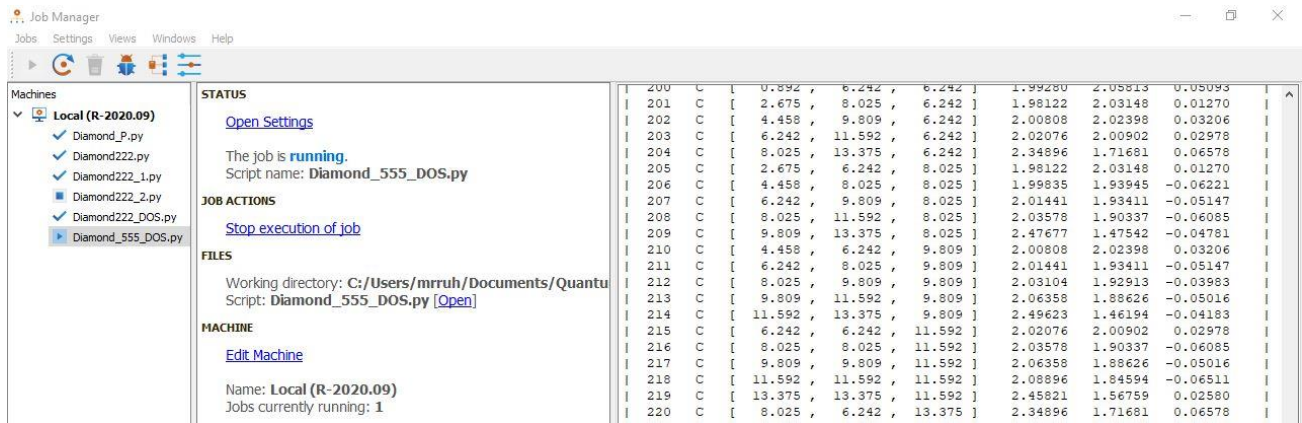


Fig. 3.1.3. Job Manager, QuantumATK.

3.2. The structure of diamond.

In this thesis, the NV center is being made inside of a cluster. First of all, the diamond cluster is figured out and paid attention to its properties. The pure diamond cluster is made by C atoms, dimensions are 5 atoms, 5 atoms, and 5 atoms through X, Y, and Z axes, respectively.

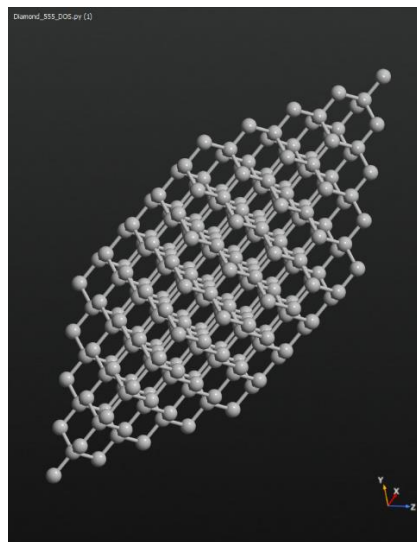


Fig.3.2.1. The diamond molecule consists of 250 C atoms.

Via LCAO calculator, the cluster of diamond is calculating. The result of Molecular Energy Spectrum and Density of State are taken for pure diamond molecule in Fig.3.2.2.

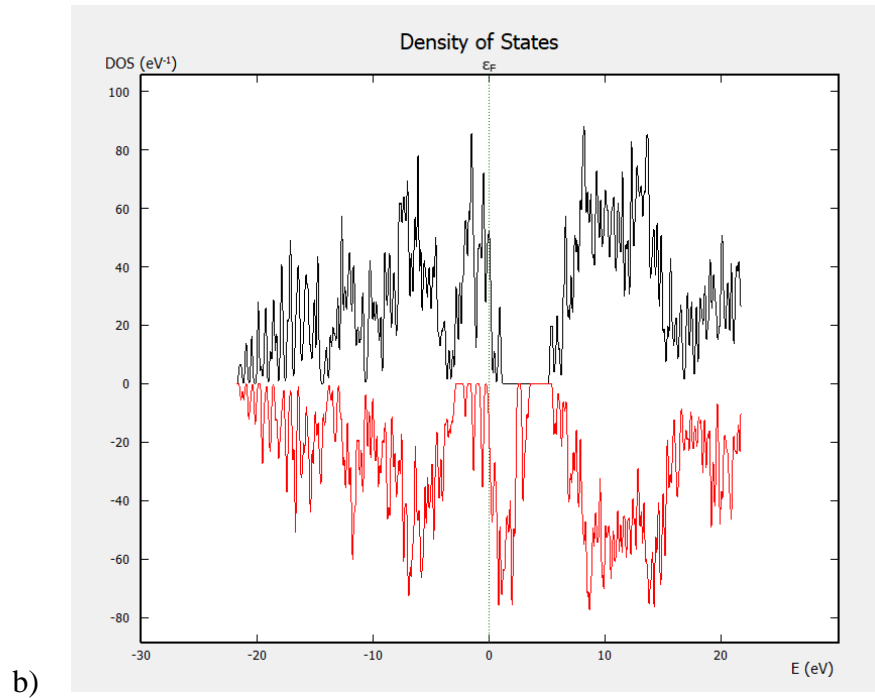
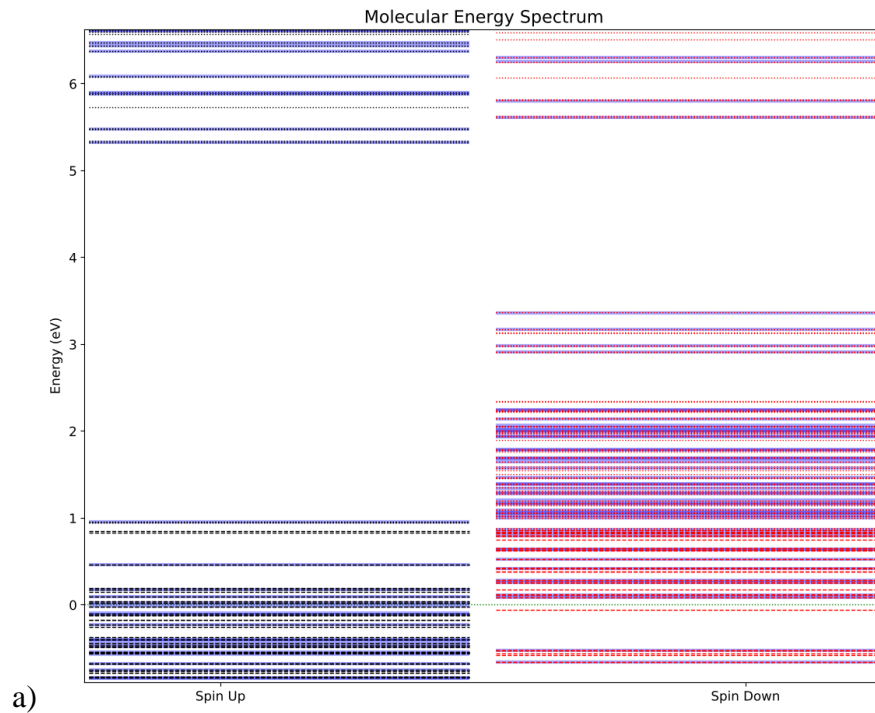


Fig. 3.2.2. (a) Molecular Energy Spectrum, (b) Density of States of diamond (black is for spin up, red is for spin down).

3.3. Diamond with Nitrogen

After this process, the N is implementing inside of a diamond. C number 187 of the molecule is changed by N. There are neighbors C numbers with N are 62, 63, 87, 67 for C1, C2, C3, C4, respectively. After the calculation molecular energy spectrum was taken for individually C atoms and N in Fig. 3.3.1. As well total DOS result is shown in Fig. 3.3.2.

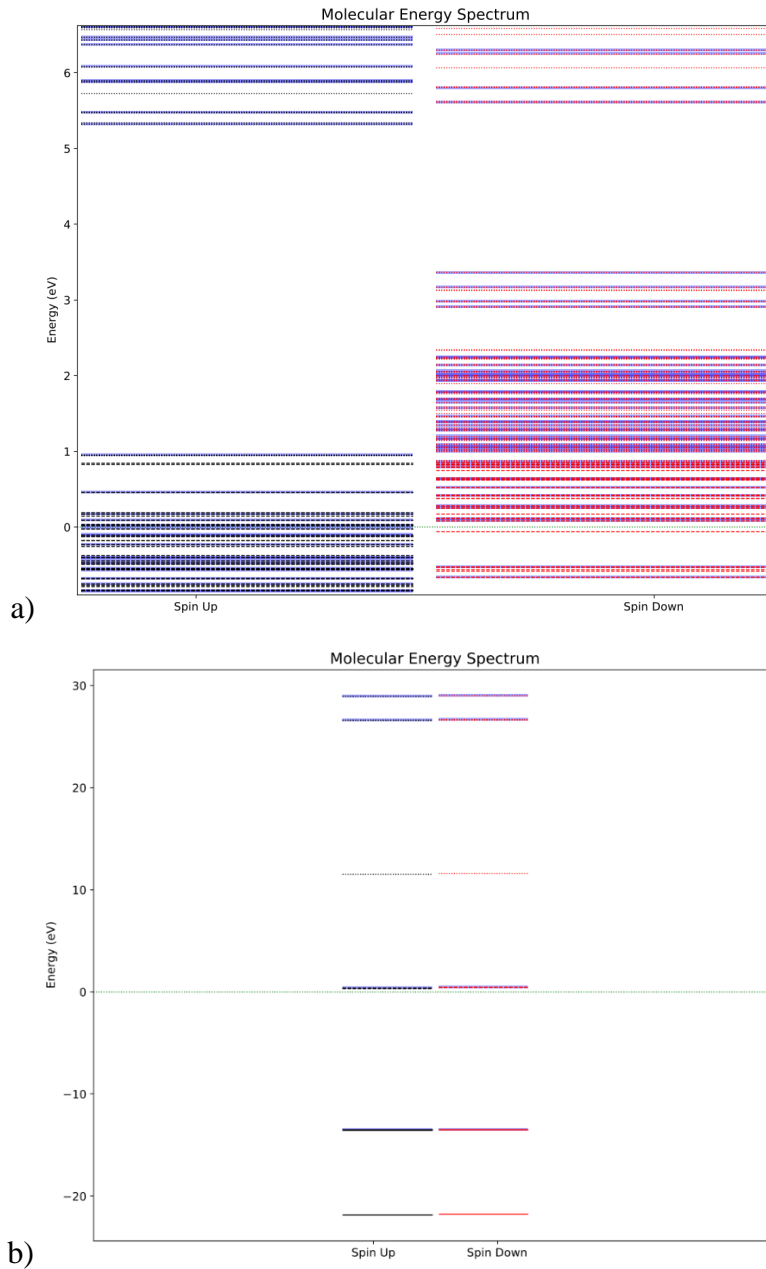


Fig. 3.2.1. (a) MES of Carbon atoms and (b) MES of Nitrogen atom.

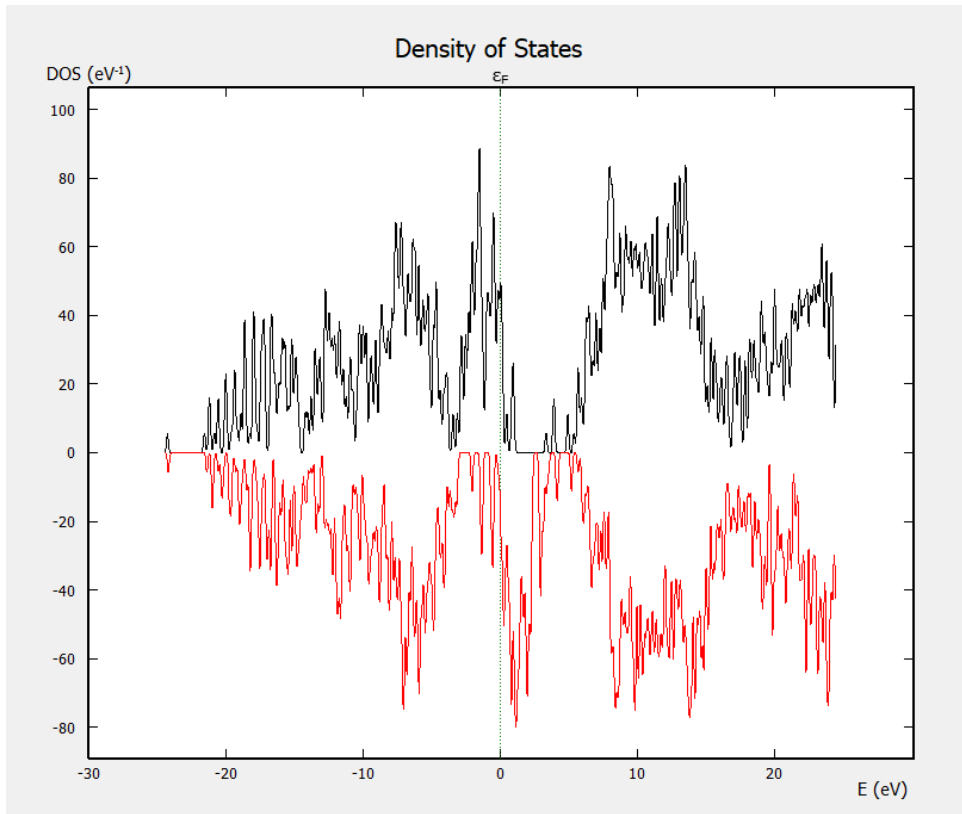


Fig. 3.3.2. Total Density of States (black is for spin up, red is for spin down).

3.4. NV center in a Diamond.

In this step, the Vacancy is created inside of the molecule and makes neighbor with nitrogen directly. This is happening with choosing one C atom which is neighbor with nitrogen and it is being deleted, the result gives us vacancy close to the N. In the 250 atoms molecule turn 249 atoms with 248 C atoms and 1 N atom. In this work, C number 62 (C1) is deleting, and neighbor C atoms with vacancy are number 185, 161, 181 which are C5, C6, C7, respectively Fig.3.3.3.

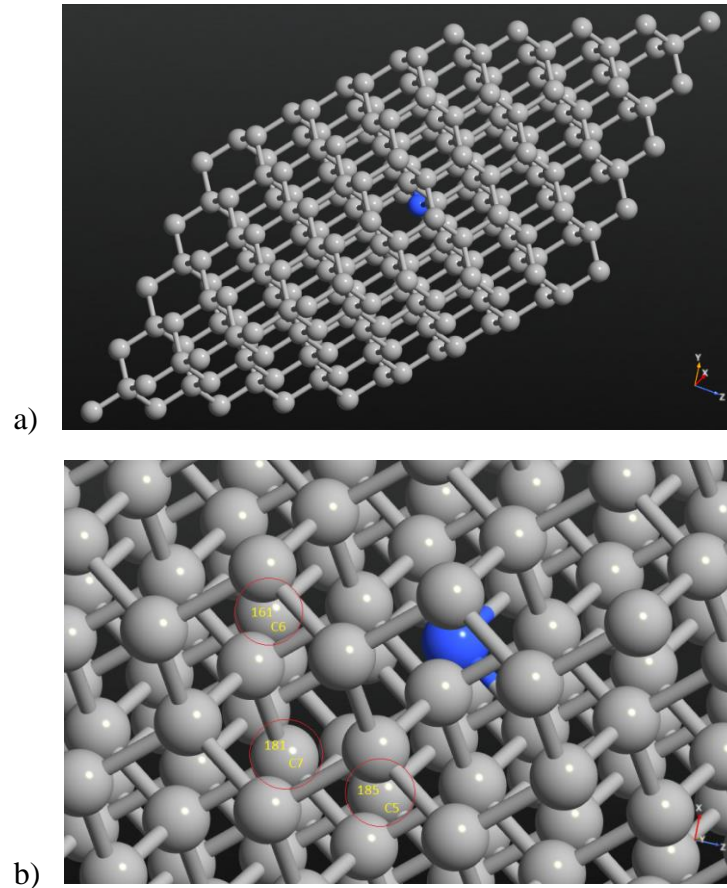
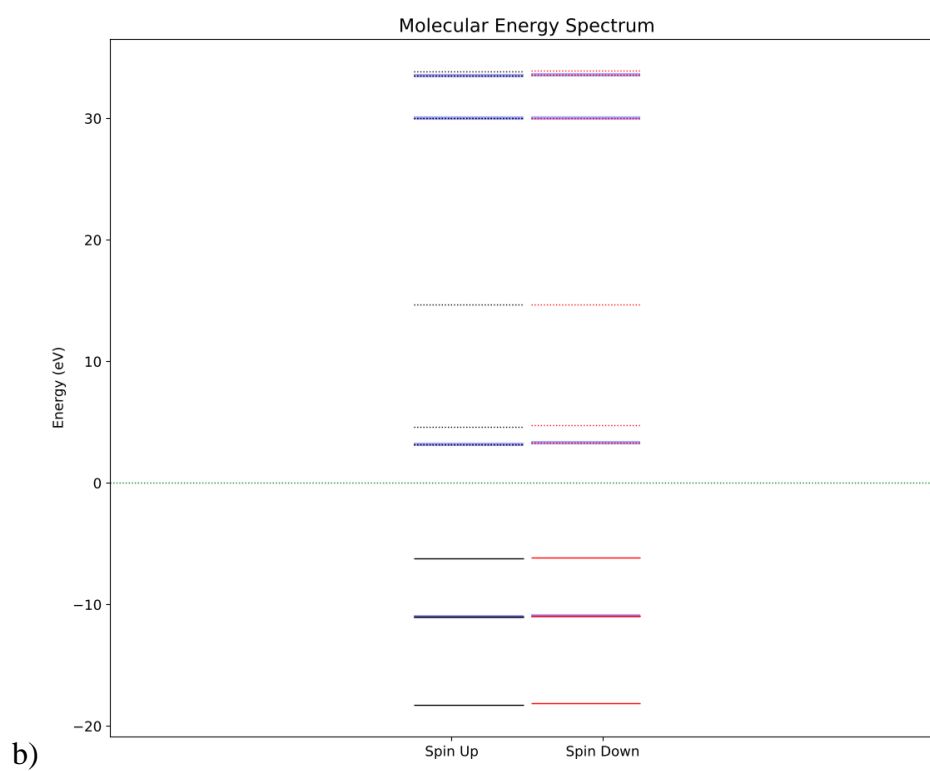
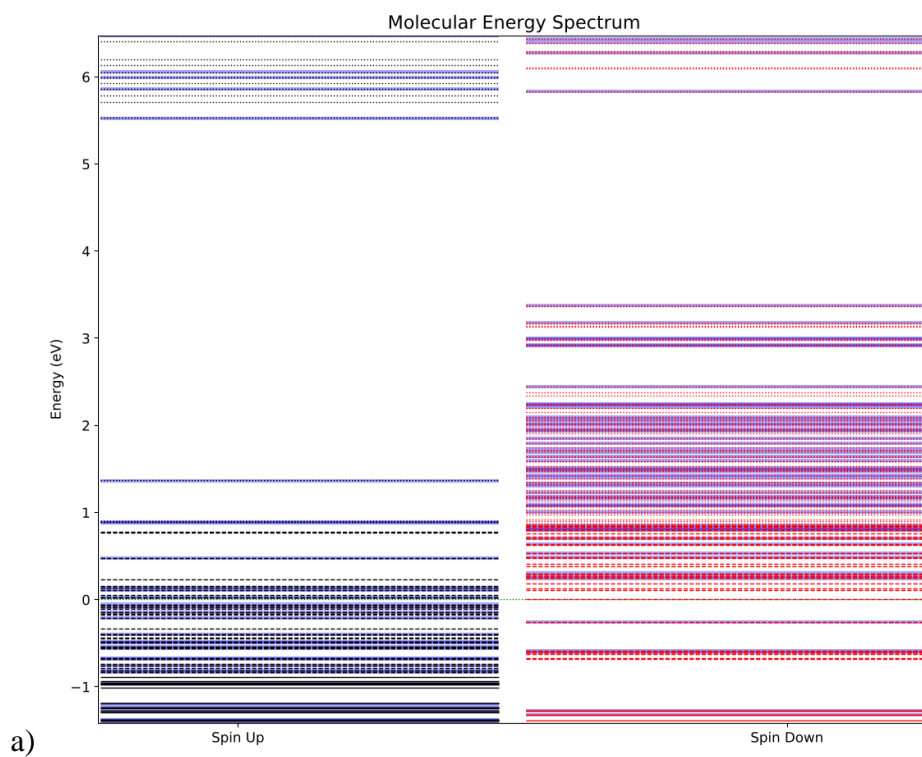


Fig. 3.3.3. (a) NV center in a diamond and (b) neighbor atoms of vacancy.

Computation starts with setting up the LCAO calculator. Polarization is chosen for spin and SGGA is chosen for exchange-correlation under the DFT-PBE method. For Pseudopotential, PseudoDojo has selected what this method supports GGA and its Cutoff value is 30-125 Ha, accuracy is High and efficiency is medium [40]. This work's density mesh cutoff is equal to 75 Hartree, occupation is Fermi-Dirac. GGA-1/2 is selected for this work as well since, in local and semi-local exchange-correlation, this method is a semi-experimental way to correct the self-interaction error [41]. For the boundary conditions Dirichlet method is used. After the computation, the MES of diamond and N and total Density of States result is shown in Fig. 3.3.4.



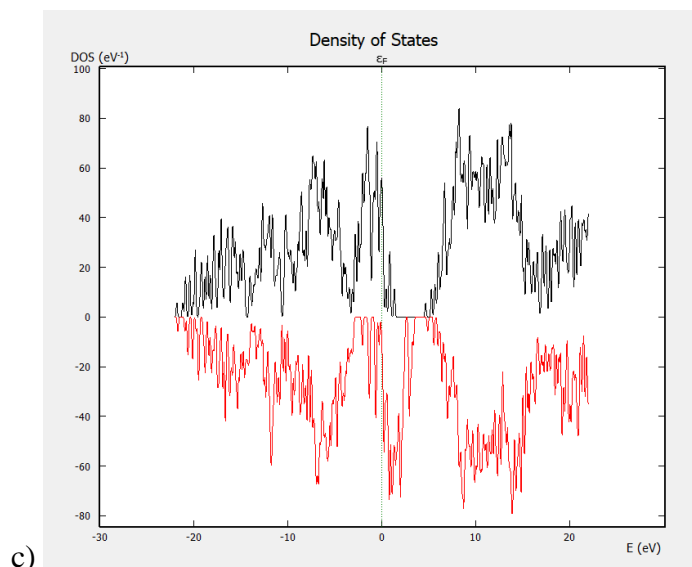


Fig. 3.3.4. (a) Molecular energy spectrum for diamond, (b) Molecular energy spectrum for Nitrogen and (c) total Density of States (black is for spin up, red is for spin down).

3.5. Optimizing of NV center

In optimization, methods are almost used the same but only GGA -1/2 is not enabled for [46]. After implementing N and take off one C, due to being of vacancy and the different sizes of N atom, the molecule size could be optimized to get appropriate bond numbers. All sides of the molecule are chosen and constraint is fixed for boundary condition from Constraints Editor in QuantumATK.

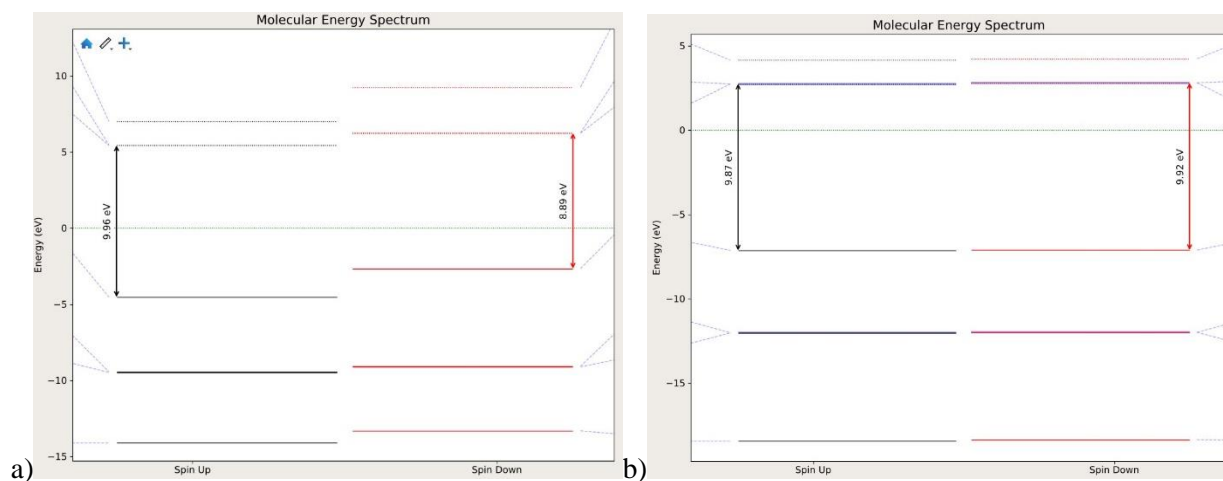


Fig.3.5.1. (a) MES of Carbon atom (C 163), (b) N atom in NV center in diamond after optimization.

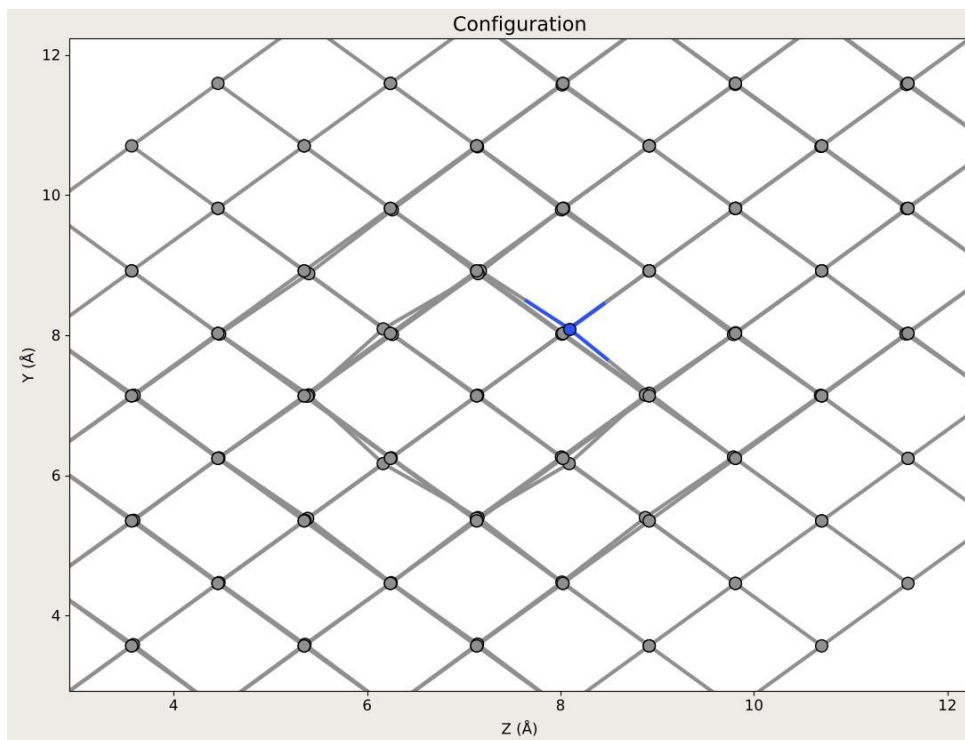


Fig.3.5.2. Changing of distance between atoms near to NV center after optimization.

<i>Atomic pair (number of position)</i>	<i>Distance Å</i>	<i>Distance Å</i>
	<i>Before optimization</i>	<i>After optimization</i>
N – C(181)	2.52	2.72
N – C(161)	2.52	2.72
N – C(185)	2.52	2.72
N – C(62)	1.54447	1.48645
N – C(66)	1.54447	1.48646
N – C(86)	1.54447	1.48645
C(181) – C(81)	1.54447	1.47463
C(181) – C(57)	1.54447	1.46331
C(181) – C(58)	1.54447	1.47464
C(66) – C(191)	1.54447	1.52959
C(66) – C(166)	1.54447	1.55216
C(66) – C(190)	1.54447	1.55216

Table 4. Interatomic distances before and after the geometry optimization. Note the increased N–C(181, 161, 185) bond lengths by approximately 8%.

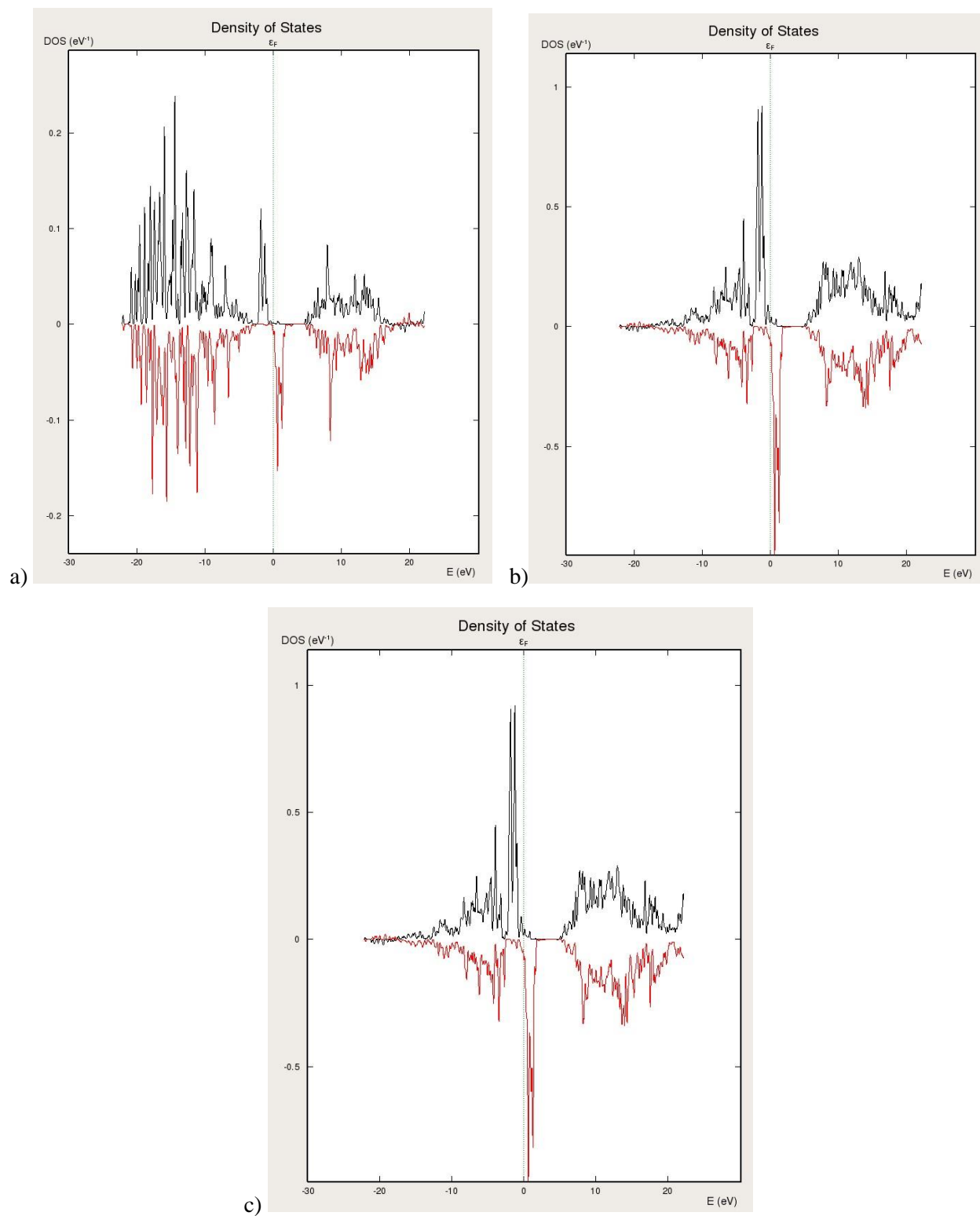


Fig.3.5.3. Density of States is for different orbitals of C (163) atom which is close to N. (a) DOS is for s orbital, (b) for p orbital, and (c) for s, p, d orbitals.

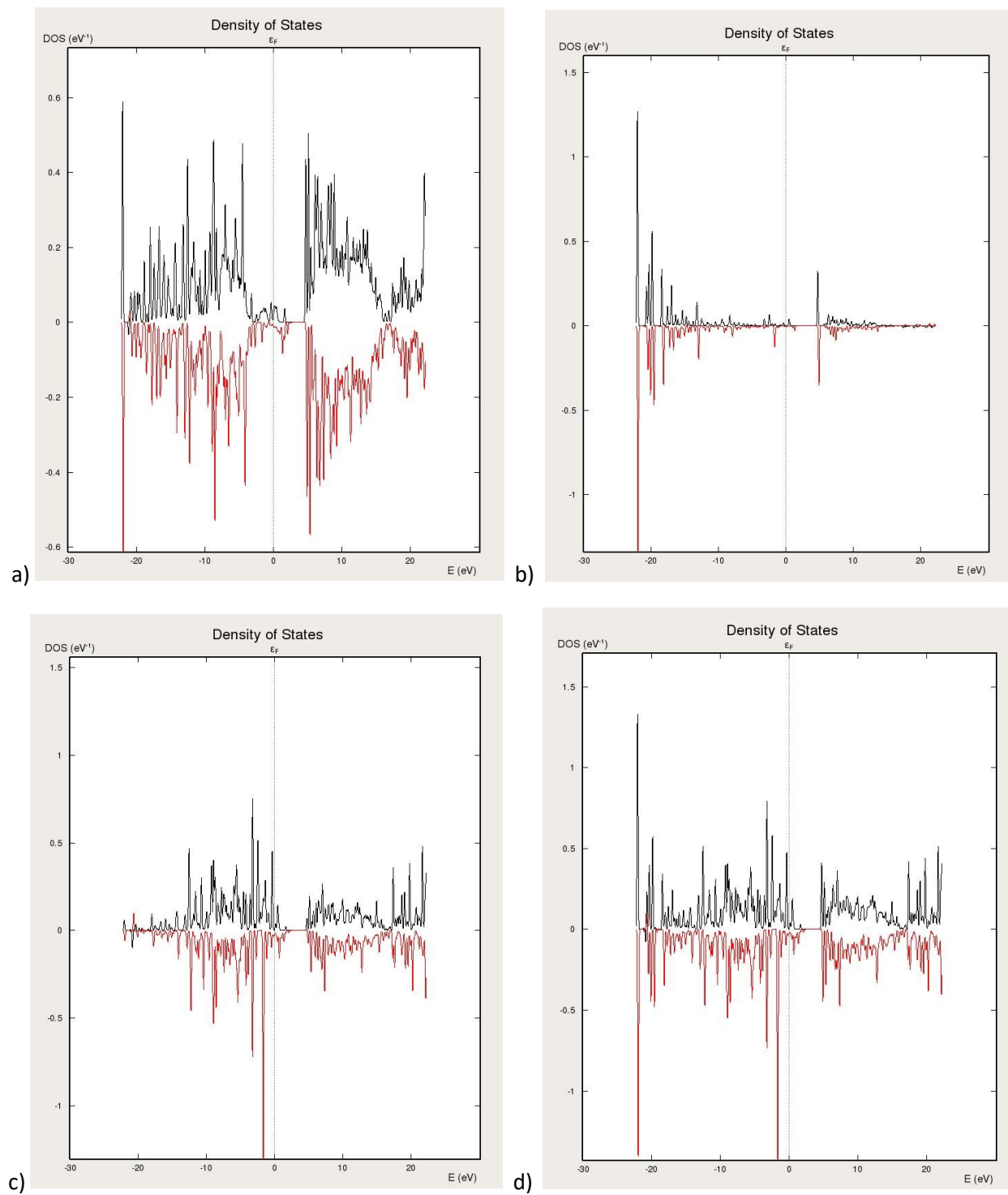


Fig.3.5.4. Density of States for C (62) atom which is neighbor of N and different orbitals of N atom. (a) DOS is for s, p, d orbitals of C (62) atom, (b) for s orbital, (c) for p orbital, and (d) for s, p, d orbital of N atom.

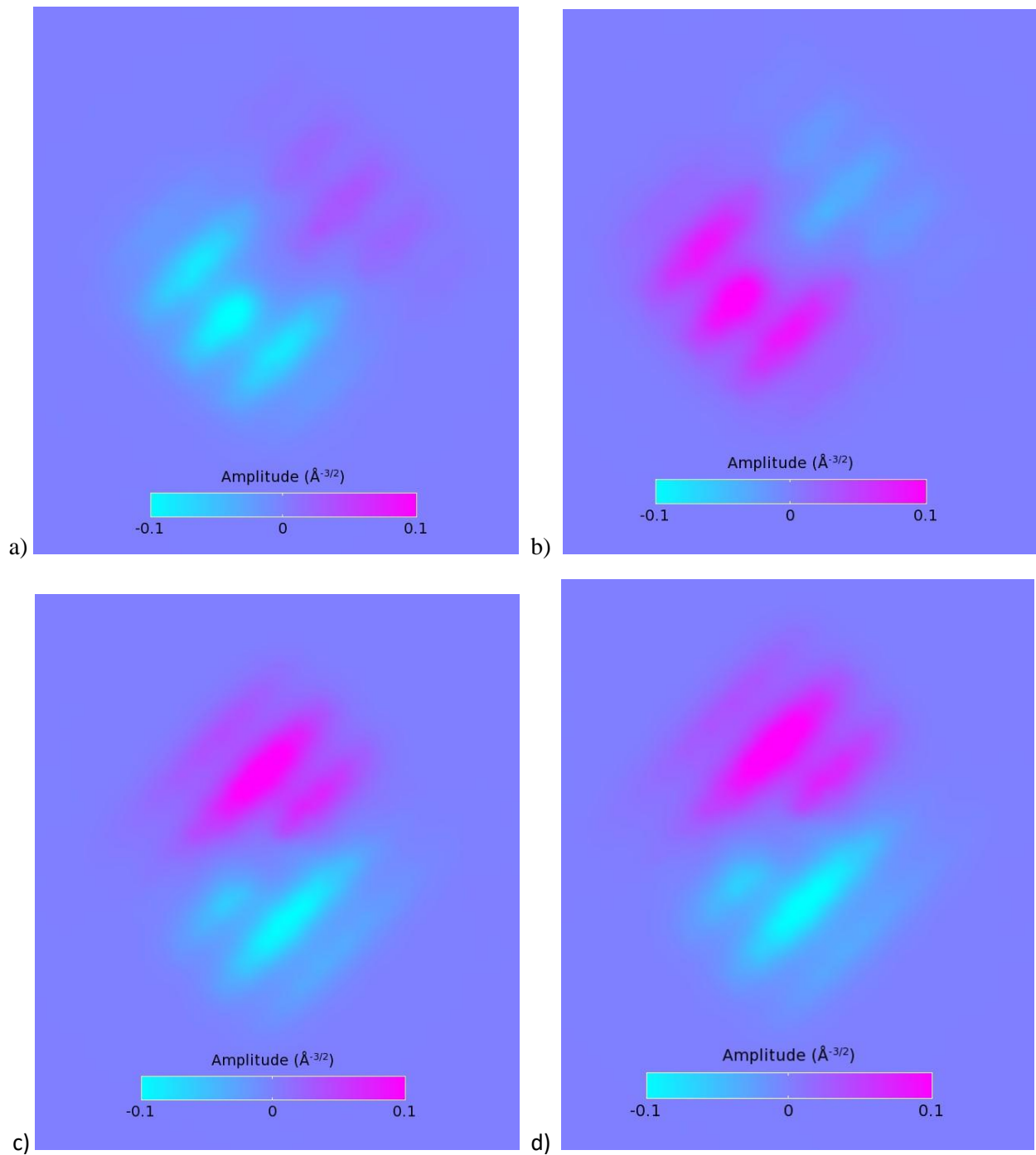


Fig.3.5.5. Eigenstates for N atom with different quantum numbers. For quantum number is 1, (a) spin-up, (b) spin-down, and for quantum number is 2, (c) spin-up, (d) spin-down.

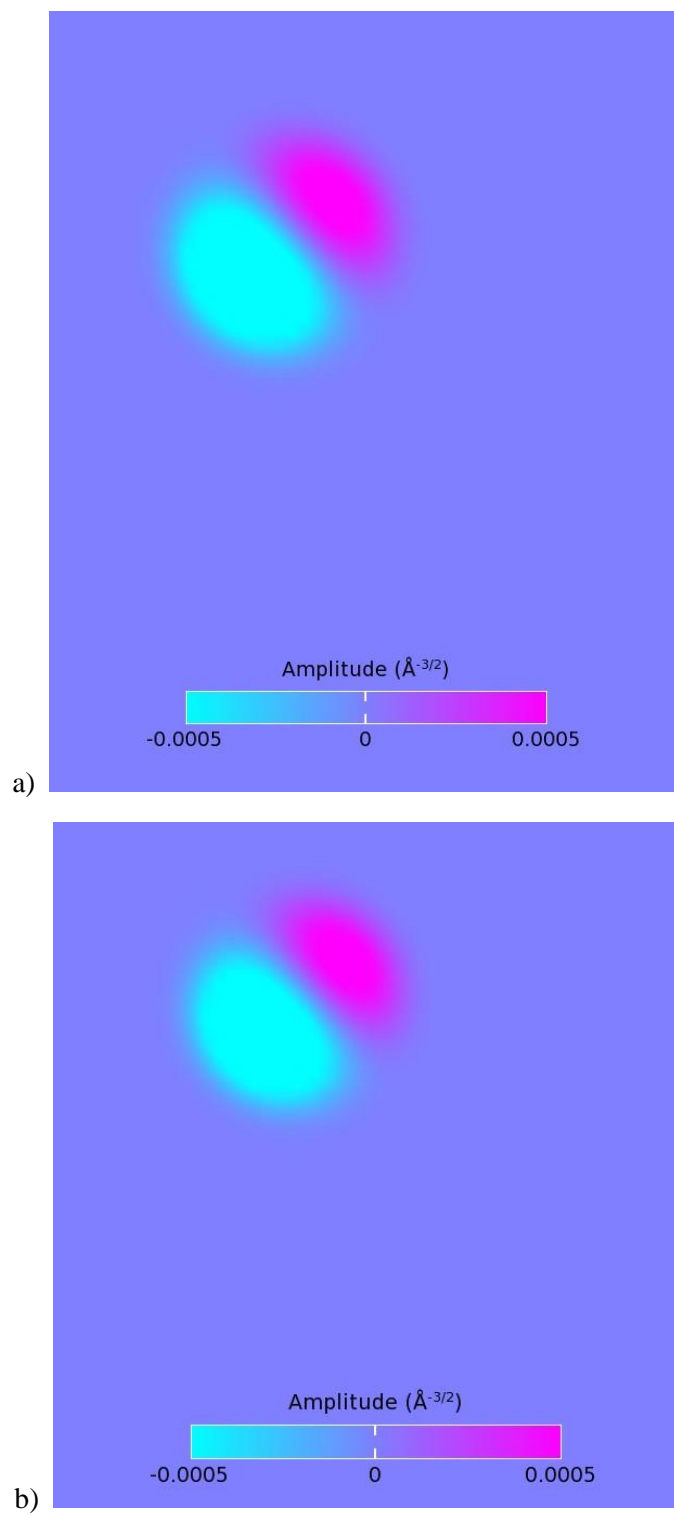


Fig.3.5.6. Eigenstates for only spin-up of C (163) atoms with quantum number is 4 (a) and 5 (b).

Results and discussion.

In this paper, NV defect was tried to create by 250 C atoms and one N atom. The size of the cluster is around 2.6 nm and bond size between atoms is 1.54447Å and the distance between N and C atoms nearest to the vacancy is 2.52 Å without optimization. According to the steps of the work and their results, the molecular energy spectrum for pure diamond HOMO-LUMO is 4.3 eV for a spin up and 2.5 eV for a spin down above the Fermi level. If it is compared DOS for a pure diamond between Fig.2.2.6. (b) which is the total density of states and Fig.3.2.2. (b), it could be seen as a result of the spin-up of Fig.3.2.2. (b) is more related to other practical work that is around 4.7 eV in above the Fermi level in Fig. 2.2.6 (b).

For the N is in the diamond gives some results that molecular energy spectrum for C, HOMO-LUMO is approximately 4 eV for spin up and 2 eV for a spin down in above the Fermi level. MES for the N, HOMO-LUMO is around 12 eV in above Fermi level. It is a higher value than Fig. 2.2.6. (a). The density of states could be compared with other work in Fig.2.2.6. (c) has around 3.5 eV band-gap total, for the Fig.3.3.2., total DOS for spin-up is related again but with more impurity which made by N.

MES for C, HOMO-LUMO is approximately 4.2 eV for spin up and 2.4 eV for a spin down in above Fermi level for NV center in diamond. But molecular energy spectrum for N, HOMO-LUMO is around 3.4 eV for spin-up/down in above the Fermi level. In the Fig.2.2.5. (b), total DOS is shown and for a spin up the bandgap is 3 eV and for a spin down the bandgap is around 3.5 eV above Fermi level. The bandgap is starting from 0.2 eV for spin up, 0.8 eV for spin down in the valence band. But in this work band gap is starting from 1.3 eV for spin up, 4.5 eV for spin down in the valence band.

After optimization of calculation, HOMO-LUMO is 9.96 eV for spin up and 8.89 eV for a spin down for one Carbon atom (C 163), and 9.87 eV for spin up and 9.92 eV for a spin down for N in a diamond with NV center according to Fig.3.5.1. If this result would be compared with the result before optimization for N atom, it could be seen there is a tiny increase of HOMO-LUMO value for optimization (comparison Fig.3.3.4 (b) and Fig.3.5.1 (b)).

Conclusion

In the theoretical part, I have touched on the power positions of qubits and tried to give an explanation of all power positions. Next, I have tried to show the role of qubits in quantum computers and how do they work in general. There is a special programming language for manage codes for QCs and I have demonstrated the relationship between qubits positions and codes for them. Also, QPU which is the brain of QCs, its material, basis, and relation with CPU was touched in this paper.

Subsequently, quantum dots which are for qubits were discussed, in this thesis, on their different building material and forming methods. The working principle of dots, properties that distinguish them from normal electronics are available in this work.

In the next part, I made a research based on the literature dealing with computation methods and results that will be comparable with this work.

In a practical part, I started with giving some basics about the QuantumATK tool that is used for this work. Then, a diamond molecule which consists of 250 C atoms was built and got its MES and DOS plot results. The result was not what I expected. Especially, HOMO-LUMO for a spin down gave much less result contrary to what I thought. In the next step, the calculation was started for diamond where N has implemented. The result was not heartwarming again, but impurity was felt by seeing reduce of the HOMO-LUMO value. When my results were compared with other works, the serious differences would be seen obviously. In the last steps, there is the calculation for NV defect in a diamond with the DFT-PBE-SGGA method, and as the result, an increase of band-gap is being observed. When I compare this result with the result of Fig.2.2.5 (b), I did not get a result which is about the similarity between spin up and down. Fermi level was not in right place in all answers. Portability, in my work I used SGGA, but in other papers mostly GGA was preferred. On other hand, the reason might be that the defects lead to cause a local shift of the Fermi level according to the literature [15].

After optimization, due to changing place of atoms, there is a force to change of distance between them. When having a look at distance values between N–C (181, 161, 185), it is possible to see an almost 8% increase of values after optimization (Table 4). This result corresponds with the published data shown in Table 2.

In conclusion, the defect that I made and the method used is not ideal, but it could be used as the starting point for a more sophisticated quantum simulation of qubits based on the NV centers in diamond.

References

- [1] Jahangir MA, Gilani SJ, Muheem A, Jafar M, Aslam M, Ansari MT, Barkat MA. Quantum Dots: Next Generation of Smart Nano-Systems. *Pharm Nanotechnol.* 2019;7(3):234-245.
- [2] Toni Kaplan. An Emerging Technology: Quantum Dots. *NMD* 102.
- [3] Reed, M. A.; Bate, R. T.; Bradshaw, K.; Duncan, W. M.; Frensley, W. R.; Lee, J. W.; Shih, H. D. "Spatial quantization in GaAs–AlGaAs multiple quantum dots". *Journal of Vacuum Science & Technology B: Microelectronics Processing and Phenomena.*
- [4] Gennady P. Berman. *Introduction to Quantum Computers.* World Scientific, 1998.
- [5] Probst CE, Zrazhevskiy P, Bagalkot V, Gao X. Quantum dots as a platform for nanoparticle drug delivery vehicle design. *Adv Drug Del Rev* 2013; 65(5): 703-18.
- [6] Andrew Steane. Quantum computing. 1998 *Rep. Prog. Phys.* 61 117.
- [7] Sergey Bravyi, David Gosset, Robert König. Quantum advantage with shallow circuits. *Science* 19 Oct 2018. Vol. 362, Issue 6412, pp. 308-311.
- [8] Keith A. Britt and Travis S. Humble. 2017. High-performance computing with quantum processing units. *J. Emerg. Technol. Comput. Syst.* 13, 3, Article 39 (March 2017), 13 pages.
- [9] M G Borselli, K Eng, R S Ross, T M Hazard, K S Holabird, B Huang, A A Kiselev, P W Deelman, L D Warren, I Milosavljevic. Undoped accumulation-mode Si/SiGe quantum dots. (August 2015).
- [10] Xin Zhang, Hai-Ou Li, Ke Wang, Gang Cao, Ming Xiao, and Guo-Ping Guo. Qubits based on semiconductor quantum dots. *Chin. Phys. B* Vol. 27, No. 2 (2018) 020305.
- [11] Li, HO., Cao, G., Yu, GD. et al. Conditional rotation of two strongly coupled semiconductor charge qubits. *Nat Commun* 6, 7681 (2015).
- [12] Daniel Loss and David P. DiVincenzo. Quantum computation with quantum dots. *Phys. Rev. A* 57, 120 – Published 1 January 1998.
- [13] Nichol, J.M., Orona, L.A., Harvey, S.P. et al. High-fidelity entangling gate for double-quantum-dot spin qubits. *npj Quantum Inf* 3, 3 (2017).
- [14] H. Kaufmann, T. Ruster, C. T. Schmiegelow, M. A. Luda, V. Kaushal, J. Schulz, D. von Lindenfels, F. Schmidt-Kaler, and U. G. Poschinger. *Phys. Rev. Lett.* 119, 150503 – Published 13 October 2017 Scalable Creation of Long-Lived Multipartite Entanglement.
- [15] Sebastien Pezzagna, Jan Meijer. Quantum computer based on color centers in diamond. Cite as: *Appl. Phys. Rev.* 8, 011308 (2021). Submitted: 22 May 2020. Accepted: 28 December 2020. Published Online: 10 February 2021.

- [16] Veldhorst, M., Eeninck, H.G.J., Yang, C.H. et al. Silicon CMOS architecture for a spin-based quantum computer. *Nat Commun* 8, 1766 (2017).
- [17] Tokuyuki Teraji. Isotopic enrichment of diamond using microwave plasma-assisted chemical vapor deposition with high carbon conversion efficiency. National Institute for Materials Science, 1-1 Namiki, Tsukuba, Ibaraki 305-0044, Japan.
- [18] Lee, SY., Widmann, M., Rendler, T. et al. Readout and control of a single nuclear spin with a metastable electron spin ancilla. *Nature Nanotech* 8, 487–492 (2013).
- [19] Jörg Wrachtrup, Fedor Jelezko. Processing quantum information in diamond. 2006 *J. Phys.: Condens. Matter* 18 S807
- [20] Roger John, Jan Lehnert, Michael Mensing, Daniel Spemann, Sébastien Pezzagna and Jan Meijer. Bright optical centre in diamond with narrow, highly polarised and nearly phonon-free fluorescence at room temperature. Roger John et al 2017 *New J. Phys.* 19 053008.
- [21] Fuchs, G., Dobrovitski, V., Toyli, D. et al. Excited-state spin coherence of a single nitrogen–vacancy centre in diamond. *Nature Phys* 6, 668–672 (2010).
- [22] J. R. Weber, W. F. Koehl, J. B. Varley, A. Janotti, B. B. Buckley, C. G. Van de Walle, and D. D. Awschalom. Quantum computing with defects. *PNAS* May 11, 2010.
- [23] T. Yamamoto, T. Umeda, K. Watanabe, S. Onoda, M. L. Markham, D. J. Twitchen, B. Naydenov, L. P. McGuinness, T. Teraji, S. Koizumi, F. Dolde, H. Fedder, J. Honert, J. Wrachtrup, T. Ohshima, F. Jelezko, and J. Isoya. Extending spin coherence times of diamond qubits by high-temperature annealing. *Phys. Rev. B* 88, 075206 – Published 23 August 2013.
- [24] Wrachtrup, J., Kilin, S.Y. & Nizovtsev, A.P. Quantum computation using the ^{13}C nuclear spins near the single NV defect center in diamond. *Opt. Spectrosc.* 91, 429–437 (2001).
- [25] Abobeih, M.H., Randall, J., Bradley, C.E. et al. Atomic-scale imaging of a 27-nuclear-spin cluster using a quantum sensor. *Nature* 576, 411–415 (2019).
- [26] The structure made by: <http://lampx.tugraz.at/~hadley/ss1/crystalstructure/structures/diamond/diamond.php> . Last seen date: April 2021.
- [27] M. Luszczeka, R. Laskowski, P. Horodeckia. The ab initio calculations of single nitrogen–vacancy defect center in diamond. *Physica B* 348 (2004) 292–298.
- [28] P. Blaha, K. Schwarz, J. Luitz, WIEN97—A full-potential linearized augmented plane wave package for calculating crystal properties, Vienna University of Technology, Institute of Physical and Theoretical Chemistry, Vienna, Austria, 1997–2000.
- [29] R. P. Messmer and G. D. Watkins. Molecular-Orbital Treatment for Deep Levels in Semiconductors: Substitutional Nitrogen and the Lattice Vacancy in Diamond. *Phys. Rev. B* 7, 2568 – Published 15 March 1973.

- [30] M. Astier, N. Pottier, and J. C. Bourgoin. Linear-combination-of-atomic-orbitals, self-consistent-field method for the determination of the electronic structure of deep levels in semiconductors. *Phys. Rev. B* 19, 5265 – Published 15 May 1979.
- [31] A Mainwood. Relaxation about the vacancy in diamond. Citation A Mainwood 1978 *J. Phys. C: Solid State Phys.* 11 2703.
- [32] Alison Mainwood. Nitrogen and nitrogen-vacancy complexes and their formation in diamond. *Phys. Rev. B* 49, 7934 – Published 15 March 1994.
- [33] Sahoo, N., Mishra, K.C., Van Rossum, M. et al. First principles cluster investigation of electronic structure and hyperfine interaction for nitrogen in diamond. *Hyperfine Interact* 35, 701–704 (1987).
- [34] E. B. Lombardi, Alison Mainwood, K. Osuch and E. C. Reynhardt. Computational models of the single substitutional nitrogen atom in diamond. Citation E B Lombardi et al 2003 *J. Phys.: Condens. Matter* 15 3135.
- [35] S. A. Kajihara, A. Antonelli, J. Bernholc, and R. Car. Nitrogen and potential n-type dopants in diamond. *Phys. Rev. Lett.* 66, 2010 – Published 15 April 1991.
- [36] The structure made by: <https://www.synopsys.com/silicon/quantumatk.html>. Last seen date: April 2021.
- [37] <https://docs.quantumatk.com/>. Last seen date: April 2021.
- [38] Anasua Chatterjee, Paul Stevenson, Silvano De Franceschi, Andrea Morello, Nathalie de Leon, Ferdinand Kuemmeth. *Semiconductor Qubits in Practice*. Wed, 13 May 2020 19:59:34 UTC (2,648 KB).
- [39] Jens Hertkorn and Maria Fyta. Electronic features of vacancy, nitrogen, and phosphorus defects in nanodiamonds. Institute for Computational Physics, Universität Stuttgart, Allmandring 3, 70569 Stuttgart, Germany.
- [40] https://docs.quantumatk.com/downloads/atk_pseudo_basis.pdf. Last seen date: May 2021.
- [41] Karin Larsson. The Combined Influence of Dopant Species and Surface Termination on the Electronic Properties of Diamond Surfaces. Department of Chemistry-Ångström Laboratory, Uppsala University, Lägerhyddsvägen 1, 75121 Uppsala, Sweden. Received: 20 January 2020; Accepted: 9 April 2020; Published: 15 April 2020.
- [42] <https://www.ibm.com/quantum-computing/>. Last seen date: May 2021.
- [43] Keith A. Britt and Travis S. Humble. 2017. High-performance computing with quantum processing units. *J. Emerg. Technol. Comput. Syst.* 13, 3, Article 39 (March 2017), 13 pages.
- [44] Martin Schill, Ralf Messmer, Alexa Herter. *SQUID Magnetometrie*. August 2016.

[45] Introduction to the D-Wave Quantum Hardware.
<https://www.dwavesys.com/tutorials/background-reading-series/introduction-d-wave-quantum-hardware>. Last seen date: May 2021.

[46] https://docs.quantumatk.com/tutorials/dft_half_pps/dft_half_pps.html. Last seen date: May 2021.

[5.350185 , 3.56679 , 5.350185],
[7.13358 , 5.350185 , 5.350185],
[8.916975 , 7.13358 , 5.350185],
[10.70037 , 8.916975 , 5.350185],
[5.350185 , 1.783395 , 7.13358],
[7.13358 , 3.56679 , 7.13358],
[8.916975 , 5.350185 , 7.13358],
[10.70037 , 7.13358 , 7.13358],
[12.483765 , 8.916975 , 7.13358],
[7.13358 , 1.783395 , 8.916975],
[8.916975 , 3.56679 , 8.916975],
[10.70037 , 5.350185 , 8.916975],
[12.483765 , 7.13358 , 8.916975],
[14.26716 , 8.916975 , 8.916975],
[0 , 3.56679 , 3.56679],
[1.783395 , 5.350185 , 3.56679],
[3.56679 , 7.13358 , 3.56679],
[5.350185 , 8.916975 , 3.56679],
[7.13358 , 10.70037 , 3.56679],
[1.783395 , 3.56679 , 5.350185],
[3.56679 , 5.350185 , 5.350185],
[5.350185 , 7.13358 , 5.350185],
[7.13358 , 8.916975 , 5.350185],
[8.916975 , 10.70037 , 5.350185],
[3.56679 , 3.56679 , 7.13358],
[5.350185 , 5.350185 , 7.13358],
[8.916975 , 8.916975 , 7.13358],
[10.70037 , 10.70037 , 7.13358],
[5.350185 , 3.56679 , 8.916975],
[7.13358 , 5.350185 , 8.916975],
[8.916975 , 7.13358 , 8.916975],
[10.70037 , 8.916975 , 8.916975],
[12.483765 , 10.70037 , 8.916975],
[7.13358 , 3.56679 , 10.70037],
[8.916975 , 5.350185 , 10.70037],
[10.70037 , 7.13358 , 10.70037],
[12.483765 , 8.916975 , 10.70037],
[14.26716 , 10.70037 , 10.70037],
[0 , 5.350185 , 5.350185],
[1.783395 , 7.13358 , 5.350185],
[3.56679 , 8.916975 , 5.350185],

[5.350185 , 10.70037 , 5.350185],
[7.13358 , 12.483765 , 5.350185],
[1.783395 , 5.350185 , 7.13358],
[3.56679 , 7.13358 , 7.13358],
[5.350185 , 8.916975 , 7.13358],
[7.13358 , 10.70037 , 7.13358],
[8.916975 , 12.483765 , 7.13358],
[3.56679 , 5.350185 , 8.916975],
[5.350185 , 7.13358 , 8.916975],
[7.13358 , 8.916975 , 8.916975],
[8.916975 , 10.70037 , 8.916975],
[10.70037 , 12.483765 , 8.916975],
[5.350185 , 5.350185 , 10.70037],
[7.13358 , 7.13358 , 10.70037],
[8.916975 , 8.916975 , 10.70037],
[10.70037 , 10.70037 , 10.70037],
[12.483765 , 12.483765 , 10.70037],
[7.13358 , 5.350185 , 12.483765],
[8.916975 , 7.13358 , 12.483765],
[10.70037 , 8.916975 , 12.483765],
[12.483765 , 10.70037 , 12.483765],
[14.26716 , 12.483765 , 12.483765],
[0 , 7.13358 , 7.13358],
[1.783395 , 8.916975 , 7.13358],
[3.56679 , 10.70037 , 7.13358],
[5.350185 , 12.483765 , 7.13358],
[7.13358 , 14.26716 , 7.13358],
[1.783395 , 7.13358 , 8.916975],
[3.56679 , 8.916975 , 8.916975],
[5.350185 , 10.70037 , 8.916975],
[7.13358 , 12.483765 , 8.916975],
[8.916975 , 14.26716 , 8.916975],
[3.56679 , 7.13358 , 10.70037],
[5.350185 , 8.916975 , 10.70037],
[7.13358 , 10.70037 , 10.70037],
[8.916975 , 12.483765 , 10.70037],
[10.70037 , 14.26716 , 10.70037],
[5.350185 , 7.13358 , 12.483765],
[7.13358 , 8.916975 , 12.483765],
[8.916975 , 10.70037 , 12.483765],
[10.70037 , 12.483765 , 12.483765],

[12.483765 , 14.26716 , 12.483765],
[7.13358 , 7.13358 , 14.26716],
[8.916975 , 8.916975 , 14.26716],
[10.70037 , 10.70037 , 14.26716],
[12.483765 , 12.483765 , 14.26716],
[14.26716 , 14.26716 , 14.26716],
[0.8916975 , 0.8916975 , 0.8916975],
[2.6750925 , 2.6750925 , 0.8916975],
[4.4584875 , 4.4584875 , 0.8916975],
[6.2418825 , 6.2418825 , 0.8916975],
[8.0252775 , 8.0252775 , 0.8916975],
[2.6750925 , 0.8916975 , 2.6750925],
[4.4584875 , 2.6750925 , 2.6750925],
[6.2418825 , 4.4584875 , 2.6750925],
[8.0252775 , 6.2418825 , 2.6750925],
[9.8086725 , 8.0252775 , 2.6750925],
[4.4584875 , 0.8916975 , 4.4584875],
[6.2418825 , 2.6750925 , 4.4584875],
[8.0252775 , 4.4584875 , 4.4584875],
[9.8086725 , 6.2418825 , 4.4584875],
[11.5920675 , 8.0252775 , 4.4584875],
[6.2418825 , 0.8916975 , 6.2418825],
[8.0252775 , 2.6750925 , 6.2418825],
[9.8086725 , 4.4584875 , 6.2418825],
[11.5920675 , 6.2418825 , 6.2418825],
[13.3754625 , 8.0252775 , 6.2418825],
[8.0252775 , 0.8916975 , 8.0252775],
[9.8086725 , 2.6750925 , 8.0252775],
[11.5920675 , 4.4584875 , 8.0252775],
[13.3754625 , 6.2418825 , 8.0252775],
[15.1588575 , 8.0252775 , 8.0252775],
[0.8916975 , 2.6750925 , 2.6750925],
[2.6750925 , 4.4584875 , 2.6750925],
[4.4584875 , 6.2418825 , 2.6750925],
[6.2418825 , 8.0252775 , 2.6750925],
[8.0252775 , 9.8086725 , 2.6750925],
[2.6750925 , 2.6750925 , 4.4584875],
[4.4584875 , 4.4584875 , 4.4584875],
[6.2418825 , 6.2418825 , 4.4584875],
[8.0252775 , 8.0252775 , 4.4584875],
[9.8086725 , 9.8086725 , 4.4584875],

[4.4584875 , 2.6750925 , 6.2418825],
[6.2418825 , 4.4584875 , 6.2418825],
[8.0252775 , 6.2418825 , 6.2418825],
[9.8086725 , 8.0252775 , 6.2418825],
[11.5920675 , 9.8086725 , 6.2418825],
[6.2418825 , 2.6750925 , 8.0252775],
[8.0252775 , 4.4584875 , 8.0252775],
[9.8086725 , 6.2418825 , 8.0252775],
[11.5920675 , 8.0252775 , 8.0252775],
[13.3754625 , 9.8086725 , 8.0252775],
[8.0252775 , 2.6750925 , 9.8086725],
[9.8086725 , 4.4584875 , 9.8086725],
[11.5920675 , 6.2418825 , 9.8086725],
[13.3754625 , 8.0252775 , 9.8086725],
[15.1588575 , 9.8086725 , 9.8086725],
[0.8916975 , 4.4584875 , 4.4584875],
[2.6750925 , 6.2418825 , 4.4584875],
[4.4584875 , 8.0252775 , 4.4584875],
[6.2418825 , 9.8086725 , 4.4584875],
[8.0252775 , 11.5920675 , 4.4584875],
[2.6750925 , 4.4584875 , 6.2418825],
[4.4584875 , 6.2418825 , 6.2418825],
[6.2418825 , 8.0252775 , 6.2418825],
[8.0252775 , 9.8086725 , 6.2418825],
[9.8086725 , 11.5920675 , 6.2418825],
[4.4584875 , 4.4584875 , 8.0252775],
[6.2418825 , 6.2418825 , 8.0252775],
[8.0252775 , 8.0252775 , 8.0252775],
[9.8086725 , 9.8086725 , 8.0252775],
[11.5920675 , 11.5920675 , 8.0252775],
[6.2418825 , 4.4584875 , 9.8086725],
[8.0252775 , 6.2418825 , 9.8086725],
[9.8086725 , 8.0252775 , 9.8086725],
[11.5920675 , 9.8086725 , 9.8086725],
[13.3754625 , 11.5920675 , 9.8086725],
[8.0252775 , 4.4584875 , 11.5920675],
[9.8086725 , 6.2418825 , 11.5920675],
[11.5920675 , 8.0252775 , 11.5920675],
[13.3754625 , 9.8086725 , 11.5920675],
[15.1588575 , 11.5920675 , 11.5920675],
[0.8916975 , 6.2418825 , 6.2418825],

```

[ 2.6750925, 8.0252775, 6.2418825],
[ 4.4584875, 9.8086725, 6.2418825],
[ 6.2418825, 11.5920675, 6.2418825],
[ 8.0252775, 13.3754625, 6.2418825],
[ 2.6750925, 6.2418825, 8.0252775],
[ 4.4584875, 8.0252775, 8.0252775],
[ 6.2418825, 9.8086725, 8.0252775],
[ 8.0252775, 11.5920675, 8.0252775],
[ 9.8086725, 13.3754625, 8.0252775],
[ 4.4584875, 6.2418825, 9.8086725],
[ 6.2418825, 8.0252775, 9.8086725],
[ 8.0252775, 9.8086725, 9.8086725],
[ 9.8086725, 11.5920675, 9.8086725],
[ 11.5920675, 13.3754625, 9.8086725],
[ 6.2418825, 6.2418825, 11.5920675],
[ 8.0252775, 8.0252775, 11.5920675],
[ 9.8086725, 9.8086725, 11.5920675],
[ 11.5920675, 11.5920675, 11.5920675],
[ 13.3754625, 13.3754625, 11.5920675],
[ 8.0252775, 6.2418825, 13.3754625],
[ 9.8086725, 8.0252775, 13.3754625],
[ 11.5920675, 9.8086725, 13.3754625],
[ 13.3754625, 11.5920675, 13.3754625],
[ 15.1588575, 13.3754625, 13.3754625],
[ 0.8916975, 8.0252775, 8.0252775],
[ 2.6750925, 9.8086725, 8.0252775],
[ 4.4584875, 11.5920675, 8.0252775],
[ 6.2418825, 13.3754625, 8.0252775],
[ 8.0252775, 15.1588575, 8.0252775],
[ 2.6750925, 8.0252775, 9.8086725],
[ 4.4584875, 9.8086725, 9.8086725],
[ 6.2418825, 11.5920675, 9.8086725],
[ 8.0252775, 13.3754625, 9.8086725],
[ 9.8086725, 15.1588575, 9.8086725],
[ 4.4584875, 8.0252775, 11.5920675],
[ 6.2418825, 9.8086725, 11.5920675],
[ 8.0252775, 11.5920675, 11.5920675],
[ 9.8086725, 13.3754625, 11.5920675],
[ 11.5920675, 15.1588575, 11.5920675],
[ 6.2418825, 8.0252775, 13.3754625],
[ 8.0252775, 9.8086725, 13.3754625],
[ 9.8086725, 11.5920675, 13.3754625],
[ 11.5920675, 13.3754625, 13.3754625],
[ 15.1588575, 15.1588575, 15.1588575]]*Angstrom

# Set up configuration
molecule_configuration = MoleculeConfiguration(
    elements=elements,
    cartesian_coordinates=cartesian_coordinates
)

# -----
# Calculator
# -----
#-----
# Basis Set
#-----
carbon_2p = ConfinedOrbital(
    principal_quantum_number=2,
    angular_momentum=1,
    radial_cutoff_radius=4.3875*Angstrom,
    confinement_start_radius=3.51*Angstrom,
    additional_charge=0,
    confinement_strength=12.5*Hartree,
    confinement_power=2,
    radial_step_size=0.001*Bohr,
)

carbon_2p_0 = HydrogenOrbital(
    principal_quantum_number=2,
    angular_momentum=1,
    radial_cutoff_radius=4.875*Angstrom,
    confinement_start_radius=3.9*Angstrom,
    charge=1.7,
    confinement_strength=12.5*Hartree,
    confinement_power=2,
    radial_step_size=0.001*Bohr,
)

```

```

)

carbon_2s = ConfinedOrbital(
    principal_quantum_number=2,
    angular_momentum=0,
    radial_cutoff_radius=3.99609375*Angstrom,
    confinement_start_radius=3.196875*Angstrom,
    additional_charge=0,
    confinement_strength=12.5*Hartree,
    confinement_power=2,
    radial_step_size=0.001*Bohr,
)

carbon_2s_0 = HydrogenOrbital(
    principal_quantum_number=2,
    angular_momentum=0,
    radial_cutoff_radius=2.36796875*Angstrom,
    confinement_start_radius=1.894375*Angstrom,
    charge=4.9,
    confinement_strength=12.5*Hartree,
    confinement_power=2,
    radial_step_size=0.001*Bohr,
)

carbon_3d = HydrogenOrbital(
    principal_quantum_number=3,
    angular_momentum=2,
    radial_cutoff_radius=3.9478515625*Angstrom,
    confinement_start_radius=3.15828125*Angstrom,
    charge=6,
    confinement_strength=12.5*Hartree,
    confinement_power=2,
    radial_step_size=0.001*Bohr,
)

Carbon_dft_half_parameters = DFTHalfParameters(
    element=PeriodicTable.Carbon,
    half_shell_n=2,
    half_shell_l=1,
    fractional_charge=0.4,
    cutoff_radius=2.5*Bohr,
    inner_radius=0.0*Bohr,
    all_electron=True,
)

CarbonBasis = BasisSet(
    element=PeriodicTable.Carbon,
    orbitals=[carbon_2s, carbon_2p, carbon_2p_0, carbon_3d, carbon_2s_0],
    occupations=[2.0, 2.5, 0.5, -1.5, 0.5],
    hubbard_u=[0.0, 0.0, 0.0, 0.0, 0.0]*eV,
    dft_half_parameters=Carbon_dft_half_parameters,
    filling_method=SphericalSymmetric,
    onsite_spin_orbit_split=[0.0, 0.0, 0.0, 0.0, 0.0]*eV,
    pseudopotential=NormConservingPseudoPotential("normconserving/pseudodojo/gga/standard/06_C.upf", local_potential_cutoff_threshold=1e-06*Hartree, local_potential_cutoff_radius=6.0*Bohr),
)

nitrogen_2p = ConfinedOrbital(
    principal_quantum_number=2,
    angular_momentum=1,
    radial_cutoff_radius=4.49609375*Angstrom,
    confinement_start_radius=3.596875*Angstrom,
    additional_charge=0,
    confinement_strength=12.5*Hartree,
    confinement_power=2,
    radial_step_size=0.001*Bohr,
)

nitrogen_2p_0 = HydrogenOrbital(
    principal_quantum_number=2,
    angular_momentum=1,
    radial_cutoff_radius=4.608984375*Angstrom,
    confinement_start_radius=3.6871875*Angstrom,
    charge=1.8,
    confinement_strength=12.5*Hartree,
    confinement_power=2,
    radial_step_size=0.001*Bohr,
)

nitrogen_2s = ConfinedOrbital(
    principal_quantum_number=2,
    angular_momentum=0,

```

```

radial_cutoff_radius=3.5*Angstrom,
confinement_start_radius=2.8*Angstrom,
additional_charge=0,
confinement_strength=12.5*Hartree,
confinement_power=2,
radial_step_size=0.001*Bohr,
)

nitrogen_3d = HydrogenOrbital(
    principal_quantum_number=3,
    angular_momentum=2,
    radial_cutoff_radius=2.5*Angstrom,
    confinement_start_radius=2.0*Angstrom,
    charge=6.8,
    confinement_strength=12.5*Hartree,
    confinement_power=2,
    radial_step_size=0.001*Bohr,
)

nitrogen_3s = HydrogenOrbital(
    principal_quantum_number=3,
    angular_momentum=0,
    radial_cutoff_radius=3.83125*Angstrom,
    confinement_start_radius=3.065*Angstrom,
    charge=5.8,
    confinement_strength=12.5*Hartree,
    confinement_power=2,
    radial_step_size=0.001*Bohr,
)

Nitrogen_dft_half_parameters = DFTHalfParameters(
    element=PeriodicTable.Nitrogen,
    half_shell_n=2,
    half_shell_l=1,
    fractional_charge=0.4,
    cutoff_radius=3.0*Bohr,
    inner_radius=0.0*Bohr,
    all_electron=True,
)

NitrogenBasis = BasisSet(
    element=PeriodicTable.Nitrogen,
    orbitals=[nitrogen_2s, nitrogen_2p, nitrogen_2p_0, nitrogen_3d, nitrogen_3s],
    occupations=[2.0, 3.5, -1.0, 0.0, 0.5],
    hubbard_u=[0.0, 0.0, 0.0, 0.0, 0.0]*eV,
    dft_half_parameters=Nitrogen_dft_half_parameters,
    filling_method=SphericalSymmetric,
    onsite_spin_orbit_split=[0.0, 0.0, 0.0, 0.0, 0.0]*eV,

    pseudopotential=NormConservingPseudoPotential("normconserving/pseudodojo/gga/standard/07_N.upf", local_potential_cutoff_threshold=1e-06*Hartree,
    local_potential_cutoff_radius=6.0*Bohr),

    )

basis_set = [
    CarbonBasis,
    NitrogenBasis,
]

#-----
# Exchange-Correlation
#-----
exchange_correlation = SGGAHalf.PBE

numerical_accuracy_parameters = NumericalAccuracyParameters(
    density_mesh_cutoff=75.0*Hartree,
)

iteration_control_parameters = IterationControlParameters(
    tolerance=0.001,
    max_steps=50,
)

poisson_solver = MultigridSolver(
    boundary_conditions=[[DirichletBoundaryCondition(),DirichletBoundaryCondition()],
        [DirichletBoundaryCondition(),DirichletBoundaryCondition()],
        [DirichletBoundaryCondition(),DirichletBoundaryCondition()]]
    )

calculator = LCAOCalculator(
    basis_set=basis_set,
    exchange_correlation=exchange_correlation,
    numerical_accuracy_parameters=numerical_accuracy_parameters,
    iteration_control_parameters=iteration_control_parameters,

```

```

    poisson_solver=poisson_solver,
)

molecule_configuration.setCalculator(calculator)
nlprint(molecule_configuration)
molecule_configuration.update()
nlsave('Diamond_Nitro_Vac.hdf5', molecule_configuration)

# -----
# Molecular Energy Spectrum
# -----
molecular_energy_spectrum = MolecularEnergySpectrum(
    configuration=molecule_configuration,
    energy_zero_parameter=FermiLevel,
    projection_list=ProjectionList(elements=[Carbon], angular_momenta=[0, 1, 2, 3])
)
nlsave('Diamond_Nitro_Vac.hdf5', molecular_energy_spectrum)
nlprint(molecular_energy_spectrum)

# -----
# Molecular Energy Spectrum
# -----
molecular_energy_spectrum = MolecularEnergySpectrum(
    configuration=molecule_configuration,
    energy_zero_parameter=FermiLevel,
    projection_list=ProjectionList(elements=[Nitrogen], angular_momenta=[0, 1, 2, 3])
)
nlsave('Diamond_Nitro_Vac.hdf5', molecular_energy_spectrum)
nlprint(molecular_energy_spectrum)

# -----
# Density Of States
# -----
kpoint_grid = MonkhorstPackGrid()

density_of_states = DensityOfStates(
    configuration=molecule_configuration,
    kpoints=kpoint_grid,
    energy_zero_parameter=FermiLevel,
    bands_above_fermi_level=All,
    method=Full,
)

nlsave('Diamond_Nitro_Vac.hdf5', density_of_states)
nlprint(density_of_states)

# -----
# Eigenstate
# -----
eigenstate = Eigenstate(
    configuration=molecule_configuration,
    projection_list=ProjectionList(elements=[Nitrogen], angular_momenta=[0, 1, 2, 3]),
    quantum_number=0,
)
nlsave('Diamond_Nitro_Vac.hdf5', eigenstate)

# -----
# Eigenstate
# -----
eigenstate = Eigenstate(
    configuration=molecule_configuration,
    projection_list=ProjectionList(elements=[Nitrogen], angular_momenta=[0, 1, 2, 3]),
    quantum_number=1,
)
nlsave('Diamond_Nitro_Vac.hdf5', eigenstate)

# -----
# Local Density Of States
# -----
kpoints = MonkhorstPackGrid()

local_density_of_states = LocalDensityOfStates(
    configuration=molecule_configuration,
    kpoints=kpoints,
    energies=numpy.linspace(-2, 6, 101)*eV,
    band_indices=All,
    energy_zero_parameter=FermiLevel,
    spectrum_method=GaussianBroadening(0.1*eV),
)
nlsave('Diamond_Nitro_Vac.hdf5', local_density_of_states)

```